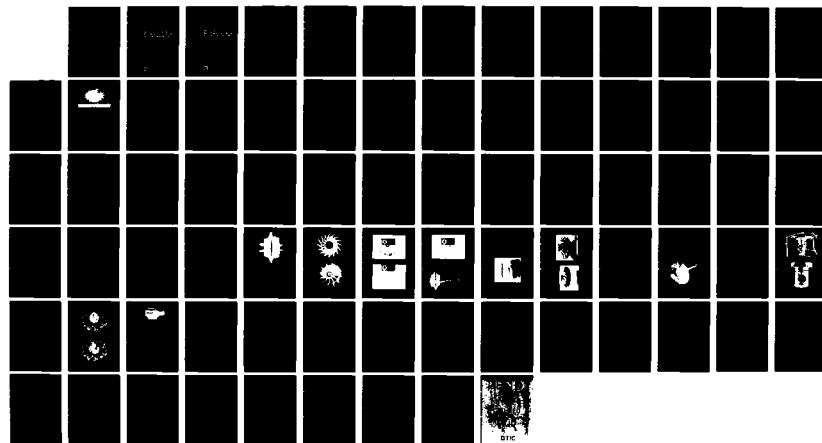
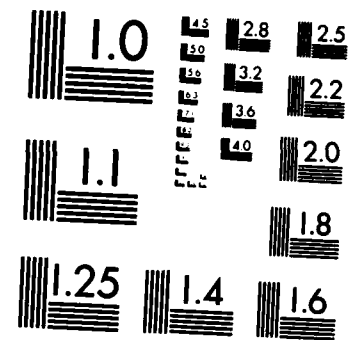


AD-A129 788 MID AND HIGH TEMPERATURE ROTOR PROGRAM FOR A 30 KW GAS  
TURBINE GENERATOR SET(U) SOLAR TURBINES INC SAN DIEGO  
CR# C RODGERS ET AL. DEC 82 ERR-0287 MERRADCOM-82472  
UNCLASSIFIED DRAK70-80-C-0152 F/G 21/5 NL 1/1





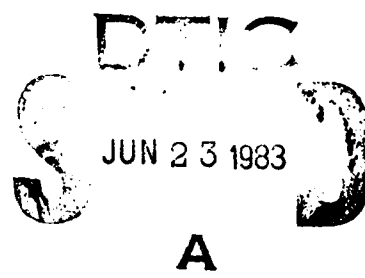
MICROCOPY RESOLUTION TEST CHART  
NATIONAL BUREAU OF STANDARDS-1963-A

DTIG FILE COPY

ADA 1239750

Final Technical Report

**Mid and High Temperature  
Rotor Program for a 30 kW  
Gas Turbine Generator Set**



This document has been approved  
for public release and sale; its  
use or disclosure is unlimited.



83 06 23 032

# Final Technical Report

## Mid and High Temperature Rotor Program for a 30 kW Gas Turbine Generator Set

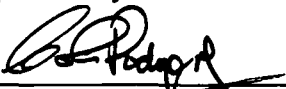
Engineering Report: ERR 0287  
Issued: December 1982

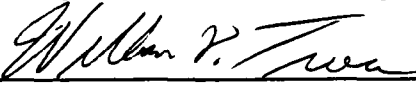
Submitted to:

U.S. Army Mobility Equipment Research  
and Development Command  
Fort Belvoir, VA 22060

Contract No.: DAAK70-80-C-0152

Prepared by:

  
C. Rodgers, Chief Analytical Engineer

  
W.D. Treece, Engineering Manager



**SOLAR  
TURBINES  
INCORPORATED**

SUBSIDIARY OF CATERPILLAR TRACTOR CO  
PO Box 80966 San Diego CA 92138

Unclassified

SECURITY CLASSIFICATION OF THIS PAGE (When Data Entered)

REPORT DOCUMENTATION PAGE		READ INSTRUCTIONS BEFORE COMPLETING FORM
1. REPORT NUMBER ERR 0287	2. GOVT ACCESSION NO. <i>100-1111-73</i>	3. RECIPIENT'S CATALOG NUMBER
4. TITLE (and Subtitle) MID AND HIGH TEMPERATURE ROTOR PROGRAM FOR A 30 KW GAS TURBINE GENERATOR SET		5. TYPE OF REPORT & PERIOD COVERED Final Report
		6. PERFORMING ORG. REPORT NUMBER 82472
7. AUTHOR(s) C. Rodgers and W. D. Treece	8. CONTRACT OR GRANT NUMBER(s) DAAK70-80-C-0152	
9. PERFORMING ORGANIZATION NAME AND ADDRESS Solar Turbines Incorporated Subsidiary of Caterpillar Tractor Co. P.O. Box 80966 San Diego, CA 92133	10. PROGRAM ELEMENT, PROJECT, TASK AREA & WORK UNIT NUMBERS	
11. CONTROLLING OFFICE NAME AND ADDRESS U.S. Army Mobility Equipment Research and Command Fort Belvoir, VA 22060	12. REPORT DATE December 1982	13. NUMBER OF PAGES 74
14. MONITORING AGENCY NAME & ADDRESS(if different from Controlling Office)	15. SECURITY CLASS. (of this report) Unclassified	
	15a. DECLASSIFICATION/DOWNGRADING SCHEDULE	
16. DISTRIBUTION STATEMENT (of this Report) Distribution of this report is unlimited.		
17. DISTRIBUTION STATEMENT (of the abstract entered in Block 20, if different from Report)		
18. SUPPLEMENTARY NOTES		
19. KEY WORDS (Continue on reverse side if necessary and identify by block number) Gas turbine, radial inflow turbine, high turbine inlet temperature, ceramic turbine, mid temperature rotor (MTR), high temperature rotor (HTR)		
20. ABSTRACT (Continue on reverse side if necessary and identify by block number) The objective of this program was the advancement of small radial inflow turbine technology in the area of operation at higher turbine inlet gas temperatures.		

Unclassified

SECURITY CLASSIFICATION OF THIS PAGE(When Data Entered)

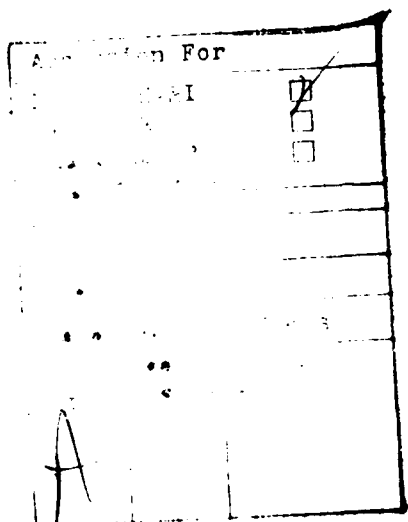
20. Abstract (Continued)

A two-phase program was structured. In the first phase, two mid-temperature range 4.50-inch tip diameter radial inflow turbine rotors, were designed for a 30-kW gas turbine with a maximum turbine inlet nozzle temperature of 2200°F. One rotor was internally air-cooled and the other conduction-cooled in a monorotor (integral turbine and compressor) arrangement. On the basis of performance, structural and cost analyses, the monorotor arrangement was selected for continued development evaluation.

A ceramic high temperature rotor was also studied for operation at a maximum turbine inlet nozzle temperature of 2600°F. Estimated failure probability for this high temperature rotor study was too high to warrant continuation.

Cast monorotors were procured during the second phase of the program. One monorotor was spin tested to 120 percent (126,000 rpm) design speed, and then intentionally burst at 135,000 rpm.

It is recommended that aerodynamic design verification testing be conducted as the next phase on the monorotor development program.



Unclassified

SECURITY CLASSIFICATION OF THIS PAGE(When Data Entered)

## CONTENTS

<b>Section</b>		<b>Page</b>
	DISCLAIMER NOTICE . . . . .	v
	ABSTRACT . . . . .	vi
1.0	INTRODUCTION . . . . .	1-1
2.0	DESIGN ANALYSIS . . . . .	2-1
2.1	TECHNOLOGY STATUS . . . . .	2-1
2.2	BASELINE CONFIGURATION . . . . .	2-2
2.3	RADIAL TURBINE DESIGN CONSTRAINTS . . . . .	2-5
2.4	EFFECT OF GEOMETRY VARIATIONS TO BASELINE ROTOR . . . . .	2-7
2.5	MTR DESIGN CONSIDERATIONS . . . . .	2-9
2.5.1	Preliminary MTR Designs . . . . .	2-11
2.6	INTERNAL-COOLED MTRS . . . . .	2-14
2.6.1	Stress and Thermal Analysis of Internally-Cooled MTR . . . . .	2-16
2.6.2	Application of Internally-Cooled MTR . . . . .	2-18
2.7	MTR MONOROTOR . . . . .	2-20
2.7.1	Thermal and Stress Analysis of MTR Monorotor . . . . .	2-21
2.7.2	Application of MTR Monorotor . . . . .	2-21
2.8	MANUFACTURING COSTS . . . . .	2-22
2.9	SELECTION OF MTR CONFIGURATION . . . . .	2-25
2.10	MTR 30-KW REGENERATIVE GENERATOR SET . . . . .	2-26
2.11	HTR DESIGN . . . . .	2-26
2.12	PHASE I DESIGN SUMMARY . . . . .	2-30
3.0	PHASE II FABRICATION . . . . .	3-1
3.1	MONOROTOR CASTINGS . . . . .	3-1
3.2	INERTIA WELDED SHAFT . . . . .	3-2
3.3	HOLOGRAPHIC TESTING . . . . .	3-6
3.4	BALANCING . . . . .	3-8
3.5	SPIN TESTING . . . . .	3-9
3.6	SUMMARY OF PHASE II TESTS . . . . .	3-15
4.0	CONCLUSIONS AND RECOMMENDATIONS . . . . .	4-1
5.0	REFERENCES . . . . .	5-1

## APPENDICES

<b>Appendix</b>		<b>Page</b>
A	CERTIFIED REPORT OF CHEMICAL ANALYSIS AND MECHANICAL TESTS . . .	A-1
B	MECHANICAL AND AERODYNAMIC DESIGN VERIFICATION TEST PLAN - MTR MONOROTOR . . . . .	B-1
C	ALTERNATE BALANCE PROCEDURE FOR SUGGESTED MONOROTOR . . . . .	C-1

## ILLUSTRATIONS

<b>Figure</b>		<b>Page</b>
2-1	Radial Turbine Cooling Technology . . . . .	2-2
2-2	Baseline Rotor Configuration . . . . .	2-3
2-3	Operating Limitations of Small Radial Turbines . . . . .	2-6
2-4	Radial Turbine Operating Limits . . . . .	2-7
2-5	Temperature Limits of Uncooled Exducer . . . . .	2-8
2-6	Superalloy Stress Rupture Limits . . . . .	2-13
2-7	MTR Design Flow Path . . . . .	2-13
2-8	MTR Internal Velocity Distributions . . . . .	2-14
2-9	MTR Preliminary Internally-Cooled Rotor . . . . .	2-15
2-10	Selected Internally-Cooled MTR Rotor . . . . .	2-16
2-11	MTR Turbine Thermal Program Inputs . . . . .	2-17
2-12	MTR Internally-Cooled Rotor Stresses . . . . .	2-18
2-13	MTR Internally-Cooled Rotor Temperatures . . . . .	2-19
2-14	40-kW Gas Turbine with Internally-Cooled Turbine Wheel . . . . .	2-19
2-15	Monorotor Preliminary Configuration . . . . .	2-20
2-16	Monorotor Tip Conditions . . . . .	2-22
2-17	Monorotor Temperature Distribution . . . . .	2-23
2-18	Final Monorotor Design . . . . .	2-23
2-19	Monorotor Equivalent Stresses . . . . .	2-24
2-20	40-kW Gas Turbine with Monorotor . . . . .	2-24
2-21	30-kW Gas Turbine with 12-Inch Regenerator Disc . . . . .	2-27
2-22	HTR Rotor Temperatures . . . . .	2-30
2-23	HTR Rotor Stresses . . . . .	2-31
3-1	Monorotor Casting . . . . .	3-2
3-2	Etching Results . . . . .	3-4
3-3	Completed Monorotor and Shaft . . . . .	3-5
3-4	Holographic Test Set-Up . . . . .	3-6
3-5	Compressor Inducer Frequency Pattern . . . . .	3-7
3-6	Turbine Exducer Frequency Pattern . . . . .	3-7
3-7	Areas of Material Removal . . . . .	3-8
3-8	Monorotor Stress Coat Spalling . . . . .	3-9
3-9	Modified Spin Fixture . . . . .	3-10
3-10	Vertical Spin Pit . . . . .	3-11
3-11	Spin Test Measurement . . . . .	3-12
3-12	Rim Fragmentation . . . . .	3-13
3-13	Shaft Shearing Due to Imbalance Forces . . . . .	3-14

## TABLES

Table		Page
2-1	Preliminary Performance Baseline for MTR and HTR Generator Sets . . . . .	2-4
2-2	Specific Weight/kW Comparison . . . . .	2-5
2-3	Major Performance Parameters of Baseline Rotor . . . . .	2-8
2-4	Effect of Geometric Parameters on Turbine Efficiency . . . . .	2-9
2-5	Preliminary MTR Design Point . . . . .	2-12
2-6	Relative Costs of Rotating Assemblies . . . . .	2-25
2-7	MTR Design Comparison . . . . .	2-26
2-8	30-kW MTR Regenerative Generator Set Performance . . . . .	2-28
2-9	HTR Design Point . . . . .	2-29
3-1	Monorotor Material Properties . . . . .	3-1

## **DISCLAIMER NOTICE**

When Government drawings, specifications, or other data are used for any purpose other than in connection with a definitely related procurement operation, the United States Government thereby incurs no responsibility nor any obligation whatsoever; and the fact that the Government may have formulated, furnished, or in any way supplied the said drawings, specifications, or other data is not to be regarded by implication or otherwise as in any manner licensing the holder or any other person or corporation, or conveying any rights or permission, to manufacture, use, or sell any patented invention that may in any way be related thereto.

The views, opinions, and/or findings contained in the report are those of the author(s) and should not be construed as an official Department of the Army position, policy, or decision, unless so designated by other documentation.

**Destroy this report when it is no longer needed.  
Do not return it to originator.**

*Distribution of this report is unlimited.*

## ABSTRACT

The objective of this program was the advancement of small radial inflow turbine technology in the area of operation at higher turbine inlet gas temperatures.

A two-phase program was structured. In the first phase, two mid-temperature range 4.50-inch tip diameter radial inflow turbine rotors, were designed for a 30-kW gas turbine with a maximum turbine inlet nozzle temperature of 2200°F. One rotor was internally air-cooled and the other conduction-cooled in a monorotor (integral/turbine and compressor) arrangement. On the basis of performance, structural and cost analyses, the monorotor arrangement was selected for continued development evaluation.

A ceramic high temperature rotor was also studied for operation at a maximum turbine inlet nozzle temperature of 2600°F. Estimated failure probability for this high temperature rotor study was too high to warrant continuation.

Cast monorotors were procured during the second phase of the program. One monorotor was spin tested to 120 percent (126,000 rpm) design speed, and then intentionally burst at 135,000 rpm.

It is recommended that aerodynamic design verification testing be conducted as the next phase on the monorotor development program.

## 1.0 INTRODUCTION

The primary objective of this program was to advance the technology of small high temperature, radial inflow turbine rotors for gas turbine generator sets in the range of 15 to 30 kW. It was required to increase rotor temperature capability, such that significant improvements in generator set thermal efficiency and power density could be attained without undue penalties in life, reliability, or cost. The baseline turbine rotor configuration selected for this program was the Turbomach T-20G generator set.

The specific objectives were design analysis and fabrication:

- **CLIN 0001 PHASE I - DESIGN ANALYSIS** - A mid-temperature rotor (MTR) will be designed for a maximum turbine nozzle inlet temperature of 2200°F representative of the threshold for simply-cooled metallic technology.

The flow path of a high temperature rotor (HTR) will be defined for a maximum turbine nozzle inlet temperature of 2600°F using ceramic material technologies realistically achievable in the 1984 to 1985 time frame or advanced cooled metallic alternates.

- **CLIN 0002 PHASE II - FABRICATION** - The MTR design will be procured in limited quantities sufficient for testing to determine mechanical integrity, including cold spin tests to verify basic design adequacy and to establish acceptance criteria.

## 2.0 DESIGN ANALYSIS

A technology status review was conducted before commencing design analysis.

### 2.1 TECHNOLOGY STATUS

To date, the following published design approaches have been analytically and experimentally investigated for small high temperature radial inflow turbines suitable for gas turbine application.

Design Approach Configuration	Reference*
1. External film cooling	1, 4
2. Internal impingement cooling	2, 4, 5
3. Disc conduction cooling	3, 4
4. Uncooled ceramic rotor	6, 7
5. Uncooled metal rotor with advanced materials	7

\*See Section 5.0

The level of cooling technology achieved is depicted in Figure 2-1. The cooling effectiveness is defined as the ratio of the difference between the relative temperature of the uncooled rotor and the local metal temperature, to the difference between the relative temperature of the uncooled rotor and the compressor discharge cooling air. Although external film cooling is effective along the back shroud and the rotor entry, rapid mixing reduces cooling effectiveness at the position of maximum blades stress.

Dependent upon the internal cooling scheme sophistication, cooling effectiveness from 40 to 60 percent is attainable. Multiple-pass cooling schemes have, however, resulted in castability problems (Ref. 1) which would become even more difficult in the smaller baseline turbine configuration.

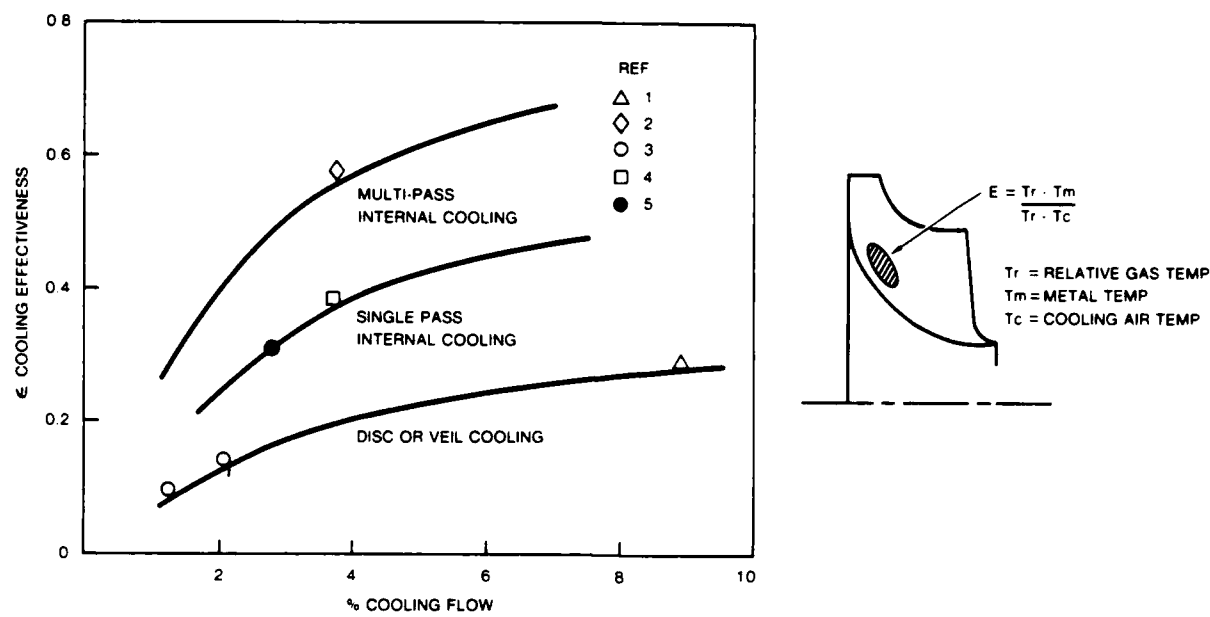


Figure 2-1. Radial Turbine Cooling Technology

## 2.2 BASELINE CONFIGURATION

The baseline configuration selected for the high temperature radial turbine program was the turbine rotor of the T-20G single-shaft gas turbine. The baseline machined rotor casting is shown in Figure 2-2, and is 4.25 inches in diameter with 18 blades. The casting is procured in MAR-M-421 and INCO 713 LC materials, dependent upon the operating environment. Engine and component performance for the T-20G, at the prescribed 5000 feet altitude and 107°F ambient temperature, is listed in Table 2-1 at the maximum rated exhaust gas temperature of 1320°F. With package inlet heating of 10°F and pressure losses of three percent, rated output power and fuel flow would be 19.8 kW and 37.2 pph respectively.

Study was required as to the possibility of uprating this baseline configuration to a mid-temperature rotor of 2200°F and a high temperature rotor of 2600°F.

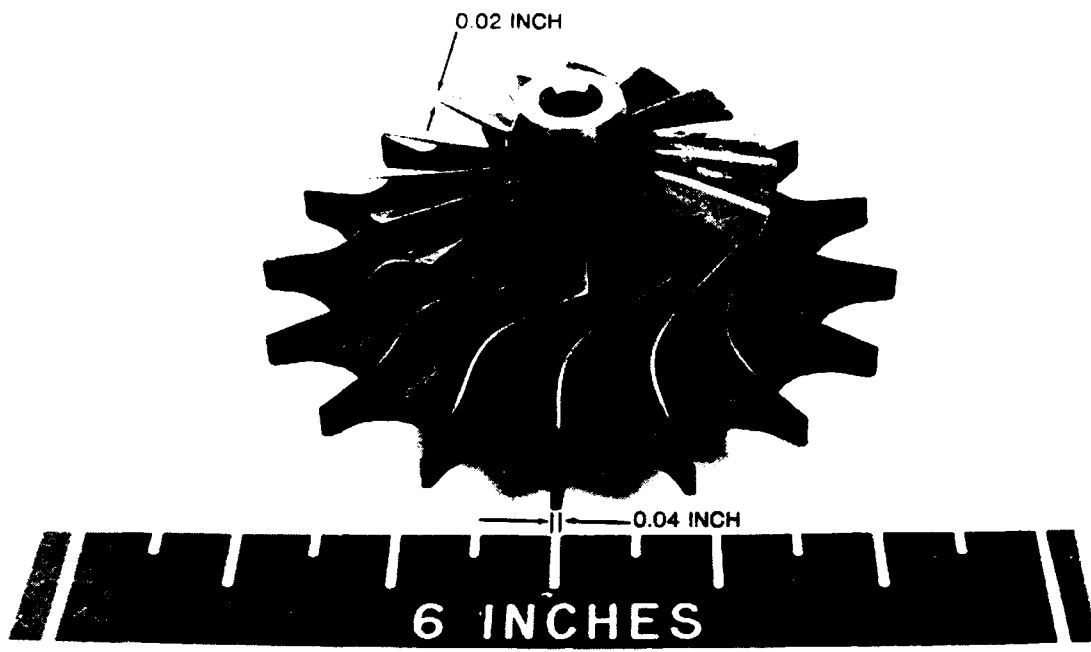


Figure 2-2. Baseline Rotor Configuration

Phase I preliminary estimates of engine performance for the uncooled MTR and ceramic HTR configurations are also included in Table 2-1 for simple-cycle and regenerative versions.

Examination of Table 2-1 data shows that significant improvements in power and specific fuel consumption are possible by increasing turbine nozzle inlet temperature up to 2200°F, if the turbine can be designed to maintain 82 percent efficiency with no significant cooling losses. Output rating could be increased to 30 kW with an advanced regenerative 2200°F T-20G generator. Increasing the turbine nozzle inlet temperature to 2600°F provides slightly more power, but no significant improvements in fuel flow.

These potential performance improvements must be weighted against the accompanying increase in cost. One such method of weighting could be the permissible cost increase to maintain the baseline generator set package's specific weight-to-power ratio (lb/kW), based upon a fly-in mission with 24-hour continuous operation at rated loads. Table 2-2 shows such a comparison, indicating that total cost increases from 50 to 100 percent for

Table 2-1. Preliminary Performance Baseline for MTR and HTR Generator Sets\*

Parameter Performance	Design Approach Configuration				
	1	2	3	4	5
Rotational Speed, krpm	93.5	105	105	105	105
Compressor Pressure Ratio	3.4	4.4	4.4	4.4	4.4
Compressor Airflow (Fixed $A_N$ ), pps	0.49	0.58	0.58	0.55	0.55
Compressor Efficiency, %	76	76	76	76	76
Package Pressure Losses, %	3	3	3	3	3
Combustor Pressure Loss, %	5	5	5	5	5
Heat Exchanger Pressure Loss, %	0	0	4.0	0	4.0
Heat Exchanger Effectiveness	0	0	0.9	0	0.9
Turbine Nozzle Inlet Temperature, °F**	1770	2200	2200	2600	2600
Turbine Tip Speed, fps	1730	2070	2050	2210	2190
Turbine Velocity Ratio	0.63	0.63	0.63	0.63	0.63
Turbine Efficiency	0.82	0.82	0.82	0.80	0.80
Turbine Exit Temperature, °F	1320	1570	1584	1887	1903
Turbine Cooling (Net Loss), %	0	0	3	0	3
Leakage, %	2	2	5	2	5
Gross Shaft Power, hp	33.3	66.0	55.0	74.7	63.2
Mechanical Losses, hp	2.0	3.0	5.0	3.0	5.0
Net Output, hp	31.3	63.0	50.0	71.7	58.2
Combustor Efficiency, %	97	97	93	97	93
Generator Efficiency, %	85	88	88	89	89
Net Output, kW	19.8	41.2	32.3	47.5	36.4
Fuel Flow (Diesel), pph	37.2	58.5	26.0	69.2	28.9
SFC, lb/kW-hr	1.87	1.42	0.81	1.45	0.76

\*5000 Feet Altitude, 107°F Ambient Temperature, 3% Pressure Losses, 10°F Inlet Heating

\*\*For preliminary design purposes, turbine nozzle inlet temperature was assumed equal to turbine rotor inlet temperature.

high temperature simple-cycle and heat-exchanged cycle engines respectively, would not be justifiable. A more reasonable cost increase would be on the order of 15 to 30 percent respectively, if technology investment is to provide a user payback.

On the basis of experience, this would translate back to the baseline turbine rotor, in fully-machined, ready-to-install condition, as a permissible cost differential of \$2000 to \$3000. This rudimentary logic series can provide a basis for the permissible degree of rotor casting sophistication.

Table 2-2. Specific Weight/kW Comparison

Parameter Performance	Design Approach Configuration				
	1	2	3	4	5
Rated Output kW	19.8	41.2	32.3	47.5	38.4
Rated Fuel Flow, pph	37.2	58.5	26.0	69.2	28.9
Package Weight, lb	460	500	560	550	610
Fuel Weight	890	1405	625	1660	695
Total Weight	1350	1905	1185	2210	1305
Specific Weight, lb/kW	68.2	46.2	36.7	46.5	34.0
Allowable Cost Increase, % (to match baseline lb/kW)	0	48	86	47	100

### 2.3 RADIAL TURBINE DESIGN CONSTRAINTS

Life Limiting Criteria are dependent upon the specific engine application and may encompass:

- Stress rupture limits
- Low cycle fatigue, and high cycle fatigue
- Environmental aspects (corrosion, oxidation, erosion)
- Disc burst speed
- Disc to shaft attachment

The particular areas of the rotor where these criteria may be life limiting are shown in Figure 2-3. For continuous-duty generator set applications (using diesel fuels), the two most significant factors are stress rupture life and environmental aspects.

Representative stress rupture limits for uncooled radial turbines are shown in Figure 2-4, and indicate that for a representative life of 500 hours at maximum temperature, it would be difficult to attain the MTR goal of 2200°F. The baseline rotor configuration exducer tip thickness of 0.020 inches is too small to allow internal cooling; thus, hot corrosion could be the limiting factor as governed by turbine exhaust gas temperature.

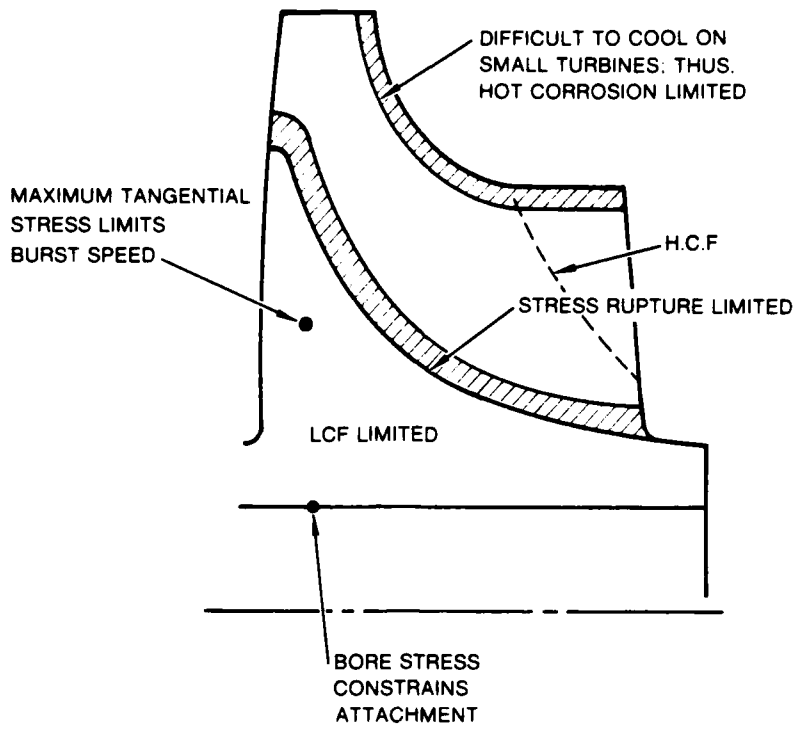


Figure 2-3. Operating Limitations of Small Radial Turbines

Figure 2-5 shows the relationship between turbine inlet temperature, turbine exhaust temperature, and compressor pressure ratio.

Pressure ratios greater than 4.0 to 1 are required to attain the MTR goal of 2200°F without exceeding a metal temperature of 1600°F in the exducer tip region.

Environmental aspects to be confronted in generator set applications are operation on diesel fuel resulting in sulfur attack and corrosion on the nozzle and rotor, plus operation in heavy dust and sand conditions. Particle ingestion with possible ensuing blockage of small cooling holes in an internally-cooled rotor could present a serious problem.

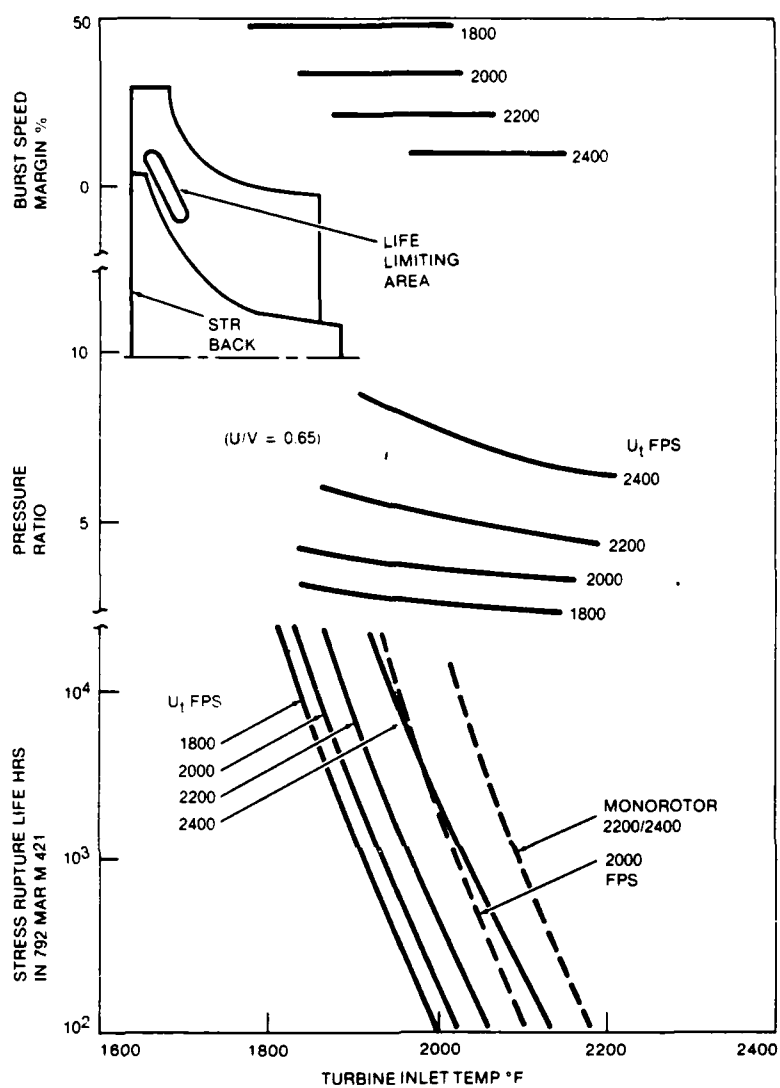


Figure 2-4. Radial Turbine Operating Limits

## 2.4 EFFECT OF GEOMETRY VARIATIONS TO BASELINE ROTOR

Major performance parameters for the baseline rotor design at the rated operating point of 5000 feet and 107°F are shown in Table 2-3. The rotor was originally designed for approximately 30 percent less flow, and a relatively high blade number was chosen for the higher blade loading.

To optimize turbine performance, blade cooling airflow must be traded against blade aerodynamic performance. This trade-off can be accomplished if cooling

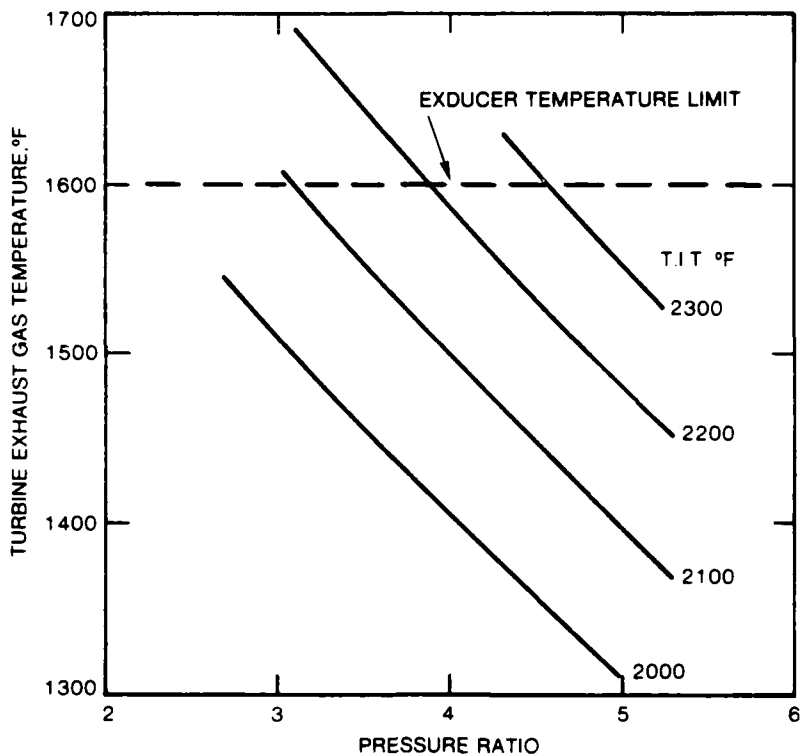


Figure 2-5. Temperature Limits of Uncooled Exducer

Table 2-3. Major Performance Parameters of Baseline Rotor

Parameters	Performance
Pressure Ratio	3.13
Rotational Speed, rpm	93,500
Airflow, pps	0.49
Flow Function $w\sqrt{T/P}$ , inlet	0.502
Efficiency (Total-Static), %	82.0
Nozzle Inlet Temperature, °F	1,770
Tip Diameter, inch	4.25
Tip Width, inch	0.24
Shroud Clearance, inch	0.035
Number of Blades	18
Exducer Shroud Diameter, inch	2.66
Exducer Hub Diameter, inch	0.87
Exducer Blade Thickness (RMS), inch	0.025
Exducer Blade Angle (RMS), degree	62
Velocity Ratio	0.63
Tip Incidence, degree	-3.0
Exit Swirl (RMS), degree	29.3

scheme effectiveness and cooling flow energy recovery are established. For preliminary purposes, the design data depicted in Figure 2-1 can be used with a conservative assumption that 50 percent of the cooling flow energy is lost.

Turbine features conducive to the reduction of cooling flow requirements are minimum surface area and increased blade thickness. The effect of these geometric parameters on turbine efficiency is shown in Table 2-4 at a velocity ratio of 0.63.

## 2.5 MTR DESIGN CONSIDERATIONS

The previous initial studies have shown that a developed MTR design would be capable of providing a generator set in the 30-kW class. The MTR design should embody the following features.

- Turbine nozzle inlet gas temperature 2200°F
- Cycle pressure ratio  $\geq 4.0$
- Blade number 12 to 14
- Higher taper ratio blades
- Tip speed 2000 to 2100 feet per second
- Fully-machined casting cost not to exceed \$2000
- Ambient conditions 5000 feet, 107°F

Table 2-4. Effect of Geometric Parameters on Turbine Efficiency

Parameters	Turbine Blade Efficiency				
Blade Number	18	16	14	12	10
$\Delta n$ , %	0.2	0	0	0.5	1.0
Exducer Thickness, inch	0.025	0.05	0.10	--	--
$\Delta n$ , %	0	1.8	4.8	--	--
Inlet Blade Height, inch	0.24	0.22	0.20	--	--
$\Delta n$ , %	0	0.2	0.8	--	--

The stage total-to-static efficiency should be 80 to 82 percent for cycle performance calculations with a minimal net cooling flow energy loss. This efficiency level is not overly conservative (as it appears) in relation to Reference 2, but is based upon practical goals for a small high temperature turbine in actual engine operation. Experience shows it is difficult to maintain tight clearance limits due to the variation in operating temperatures, operating procedures, and environments for small gas turbine generator sets.

Examination of operating conditions for other Turbomach gas turbine generator sets has shown that a viable stress rupture design life criterion is on the order of 600 hours at the maximum turbine inlet temperature occurring at 5000 feet altitude with 107°F ambient temperature condition.

The operating limits for typical radial turbines shown in Figure 2-3 indicate that it would not be possible to design an uncooled MTR to meet the 600 hour life. The MTR will, therefore, require some form of cooling.

For a tip speed of 2050 fps, the maximum blade root stress will be on the order 60 ksi. Typical superalloy stress rupture characteristics shown in Figure 2-4 indicate that with a life of 600 hours the maximum tolerable metal temperature will be approximately 1450°F.

The required cooling flow effectiveness at the blade root (near maximum radial blade height) is therefore:

$$\epsilon = \frac{1750 - 1450}{1750 - 520} = 0.25$$

The cooling flow requirements based on Figure 2-1 are:

Type of Cooling	Flow, %
Disc or veil	7
Monorotor	0
Single-pass internal cooling	2.2
Multiple-pass internal cooling	1.3

This suggests that initial recommended design solutions for a conventional superalloy MTR would be the monorotor and single-pass internal cooling approaches.

### 2.5.1 Preliminary MTR Designs

Modifications to the baseline rotor to satisfy MTR requirements are basically:

- Higher tip speed
- Reduced number of blades with higher taper ratio
- Material and cooling method selection to meet 500 hours stress rupture life.

Testing has demonstrated the feasibility of operating the engine with the rotational speed increased to 105,000 rpm. Corresponding rotor tip diameter to attain a velocity ratio of 0.63 with an expansion ratio of 4.0 would be 4.5 inches. The optimized aerodynamic design point for the MTR at these conditions is listed in Table 2-5. This design point provides initial geometric features of the MTR to permit the next design task of identifying an internal flowpath. To minimize blade stress and fabrication costs, it is customary to restrict the blade design to the radial element type with blade hub/tip taper ratios of 4.0 to 5.0. An examination of the exducer diameter ratio and speed indicated that the hub centrifugal stress would be approximately:

$$\text{HUB CF Stress} = 39.5 \left[ 1 + \left( \frac{1}{\text{Taper Ratio}} \right) \right] \text{ksi}$$

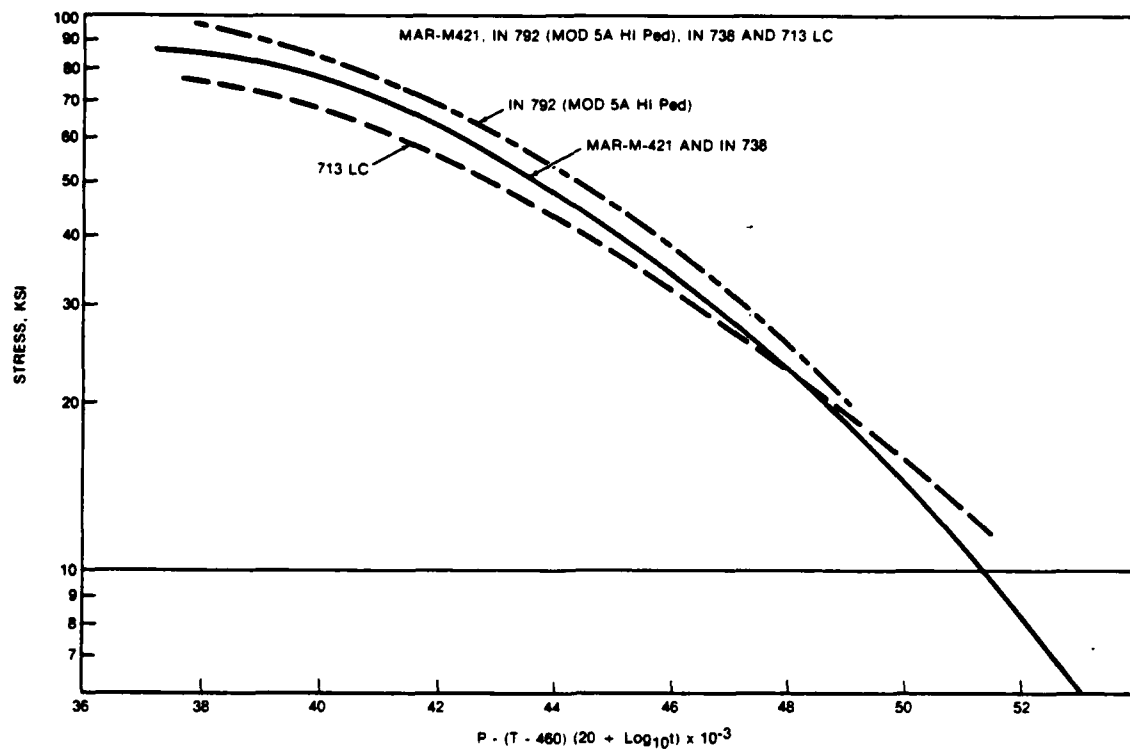
With an uncooled exducer operating with an EGT of 1580°F and designed for a life of 500 hours, a maximum blade stress of 48 ksi is permissible using the upper limit of the conventional superalloy stress rupture characteristics in Figure 2-6. A blade taper ratio of 4.0 to 5.0 was, therefore, initially selected. Note that doubling the blade taper ratio to 10 would reduce the blade root stress by 10 percent, and at the same time would incur an aerodynamic performance penalty.

Table 2-5. Preliminary MTR Design Point

Parameter	Design Point
Pressure Ratio	4.0
Rotational Speed, rpm	105,000
Airflow, pps	0.58
Nozzle Inlet Temperature, °F	2,200
Flow Function, $w\sqrt{T/P}$ , inlet	0.50
Efficiency (Total-Static), %	81
Tip Diameter, inch	4.5
Tip Speed, fps	2,060
Tip Width, inch	0.22
Shroud Clearance, inch	0.035
Number of Blades	12
Exducer Shroud Diameter, inch	2.75
Exducer Hub Diameter, inch	0.87
Exducer Blade Thickness (RMS), inch	0.035
Exducer Blade Angle (RMS), degree	56
Velocity Ratio	0.63
Tip Incidence, degree	19.0
Blade Tip Relative Temperature, °F	1,890
Exhaust Gas Temperature, °F	1,580

The previous inlet and exit flow conditions and structural considerations were used to arrive at the MTR meridional flow path and blade thicknesses shown in Figure 2-7. The requirement for radial blade elements and minimum exducer blade overlaps for castability then establishes the blade circumferential wrap. This rotor configuration was examined using the axisymmetric internal flow analysis program to assess velocity gradients and blade loading characteristics. Figure 2-8 shows the rotor internal velocity distributions along the shroud, mean, and hub stream tubes. Relatively smooth loading is observed with no regions of negative velocities.

At this point, it was possible to study the rotor cooling techniques and to reiterate the preliminary design process as necessary to formalize selected MTR final designs.



NOTES:

1. T - TIME IN HOURS
2. T - TEMPERATURE IN °F
3. MINIMUM STRENGTH VALUES SHOWN FOR DESIGN USE AT SOLAR.
4. TYPICAL VALUES REDUCED TO 80%.

5. DATA SOURCES

a. (1) MAR-M-421 MARTIN METALS TECHNICAL DATA FIGURES 3.2 AND 3.10.	b. IN 792 (-MOD 5A) HI Ped (1) R76B-4003-22 (2) R77B-4312-13
(2) ALLISON DATA (MACHINED FROM BLADES)	c. 713LC - INCO TECH. DATA 15C 10-64-4290
(3) SOLAR RDR 1675	d. IN738 - INCO TECH. DATA IM 10-68-5096
(4) AM23	

Figure 2-6. Superalloy Stress Rupture Limits

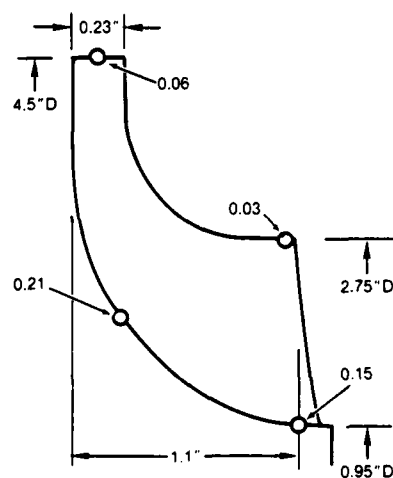


Figure 2-7. MTR Design Flow Path

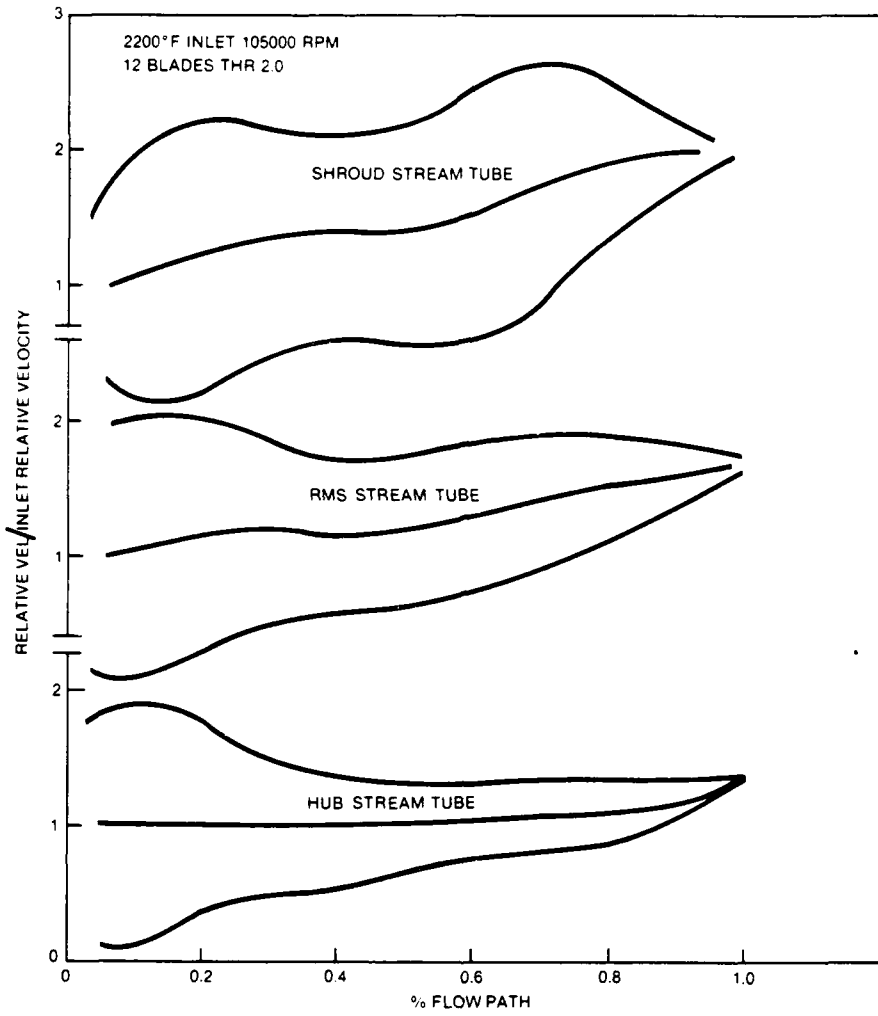


Figure 2-8. MTR Internal Velocity Distributions

## 2.6 INTERNALLY-COOLED MTRs

Several methods to internally cool radial inflow rotors have been investigated. The design shown in Figure 2-9 is different in that the revision to a previous manufacturing technique, using a two-piece rotor/exducer combination, makes it convenient to EDM axial cooling holes in the highly stressed regions of the rotor disc and blades. Circumferential alignment of the rotor-to-exducer is optimized to use ejected rotor trailing edge cooling air in addition to film cooling the exducer.

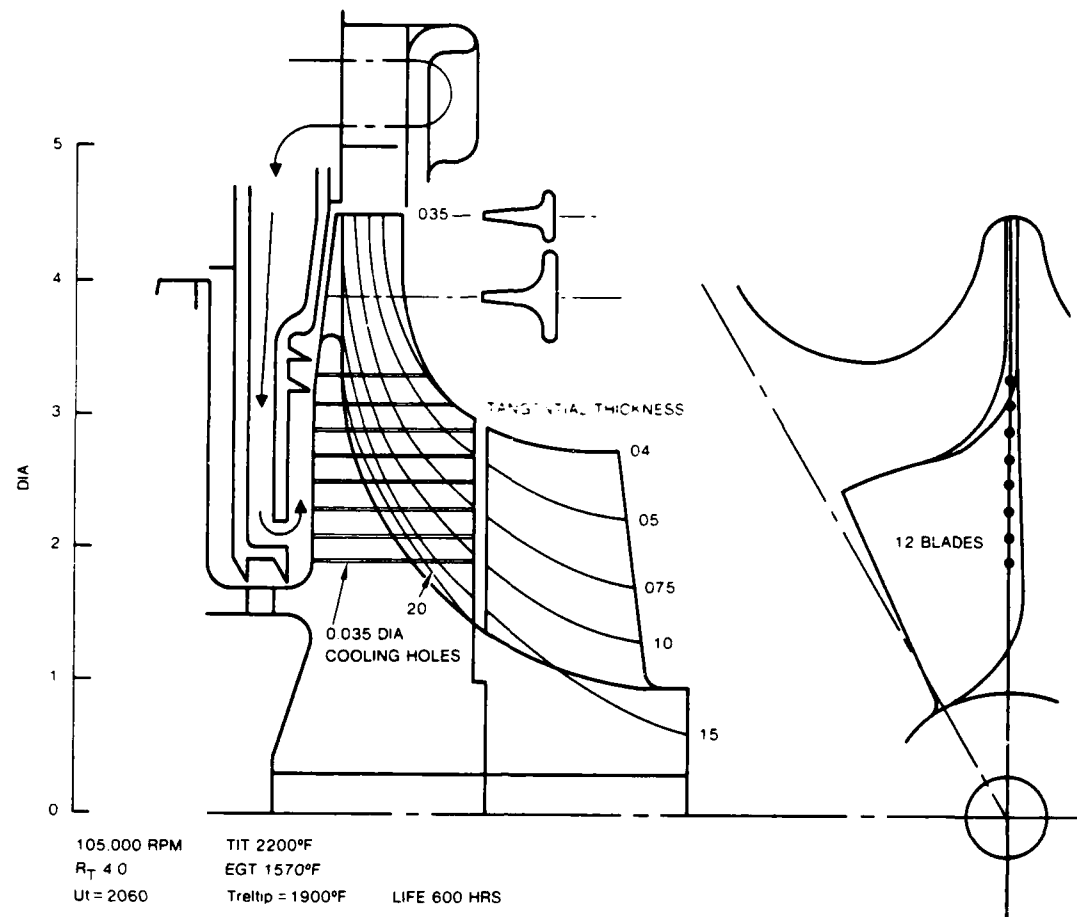


Figure 2-9. MTR Preliminary Internally-Cooled Rotor

Relatively cool compressor discharge air ( $420^{\circ}\text{F}$ ) flows down through the stationary seal plate between the compressor and turbine rotors. Compressor discharge pressure is maintained at the rotor hub by radial and axial labyrinth seals. Flow metering is accomplished by the seal gaps and cooling hole orifice sizing.

The large difference between the cooling air and rotor tip metal temperatures could provide a high radial temperature gradient and, thus, a high additive thermal stress. For 500 hours life, the blade root should be cooled to a temperature in the range of  $1350$  to  $1450^{\circ}\text{F}$ . Without any conduction down the

blade or cooling the rotor tip, metal temperature would approach the gas relative temperature of 1900°F. For the required life, the tip stress could, therefore, not exceed 10 ksi in a conventional superalloy. The alternative internally-cooled MTR design selected is shown in Figure 2-10. This design alleviated the thermal gradient problems of the previous design and also permitted cooling in the hot tip section at the expense of roughly tripling the casting manufacturing cost. Thicker blades were required to allow for the cooling passage inserts, which would result in a slight performance decrement.

### 2.6.1 Stress and Thermal Analysis of Internally-Cooled MTR

Stress analysis of the internally-cooled MTR rotor was simplified by generating equivalent mass-lumped blades attached to a disc (body of revolution) two-dimensional finite element model. The resulting blade stresses are, therefore, slightly optimistic and do not reflect stress concentration zones that would exist at internal cooling hole galley junctures. Thermal analysis was completed using the data of Figure 2-11 and a finite difference nodal network computer model. Maximum cooling flow was

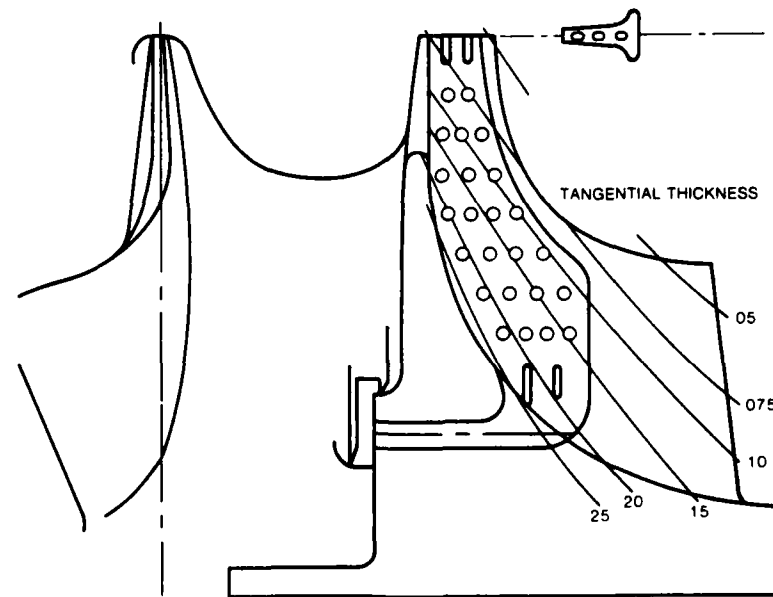


Figure 2-10. Selected Internally-Cooled MTR Rotor

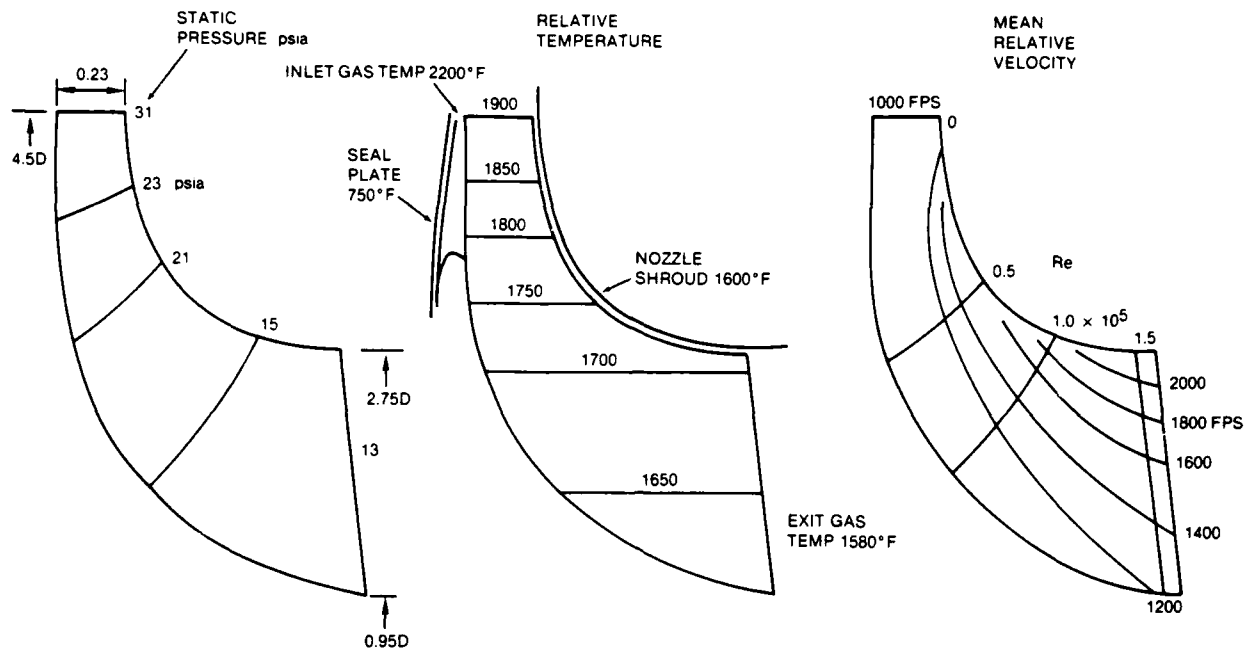


Figure 2-11. MTR Turbine Thermal Program Inputs

limited to three percent (compressor exit flow) by the size of the rotor tip cooling air ejection orifices ( $3.0 \times 0.025 \times 0.03$  sq. inches). The calculated equivalent primary cooling loss incurred by rotor pumping for tip ejection was 2.5 percent.

Rotor stresses and temperature distribution are shown in Figure 2-12 for IN 792 material. Estimated stress rupture life for the life-limiting element was 650 hours. Disc burst speed was 129 percent design speed. The steady-state design point temperature distribution shown in Figure 2-13 confirms preliminary cooling effectiveness studies (Figure 2-1) for the single-pass system. Maximum metal temperatures occur near the uncooled exducer trailing edge.

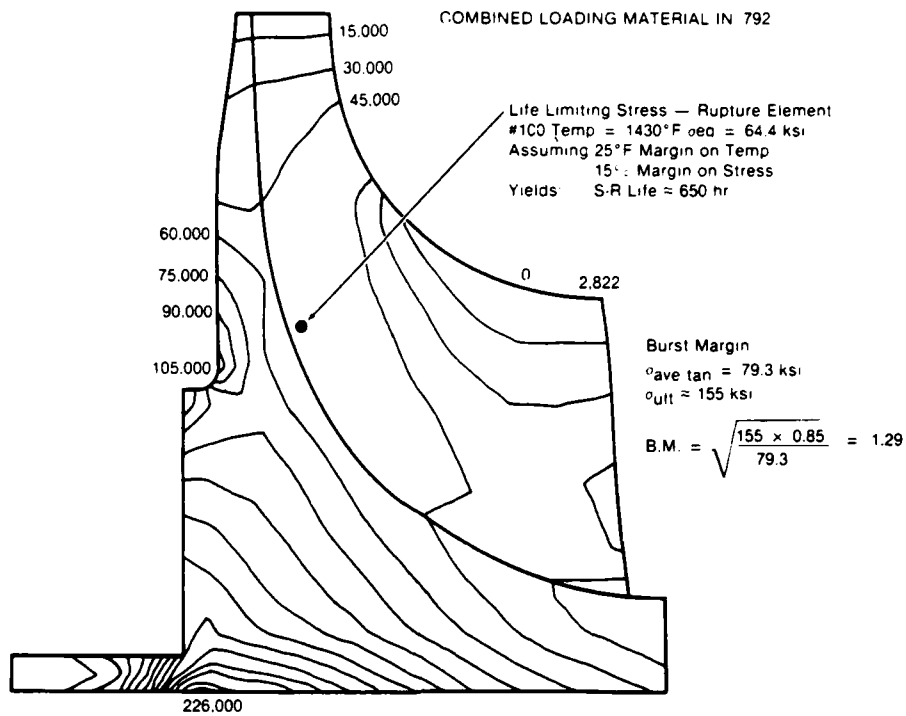


Figure 2-12. MTR Internally-Cooled Rotor Stresses

The relatively small tip ejection holes ( $0.025 \times 0.03$ ) and passage minimum width of 0.025 are of concern and could become blocked in adverse environmental operating conditions not uncommon to small portable generator sets. Small gas turbines with small fuel flows are also sensitive to fuel atomization and soot formation, and deposition could be a potential problem with the MTR internally-cooled rotor.

#### 2.6.2 Application of Internally-Cooled MTR

A small 40-kW gas turbine, simple-cycle generator set powerhead incorporating an internally-cooled MTR is depicted in Figure 2-14. Compressor discharge

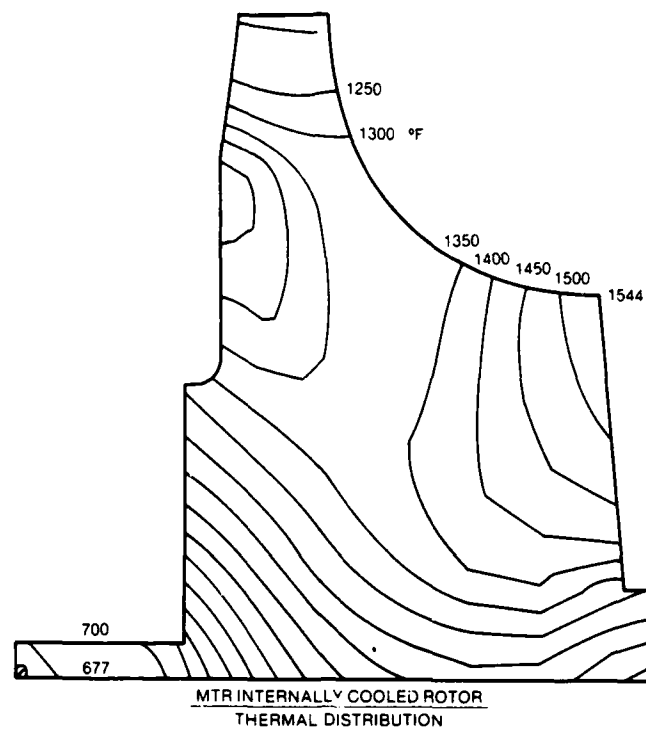


Figure 2-13. MTR Internally-Cooled Rotor Temperatures

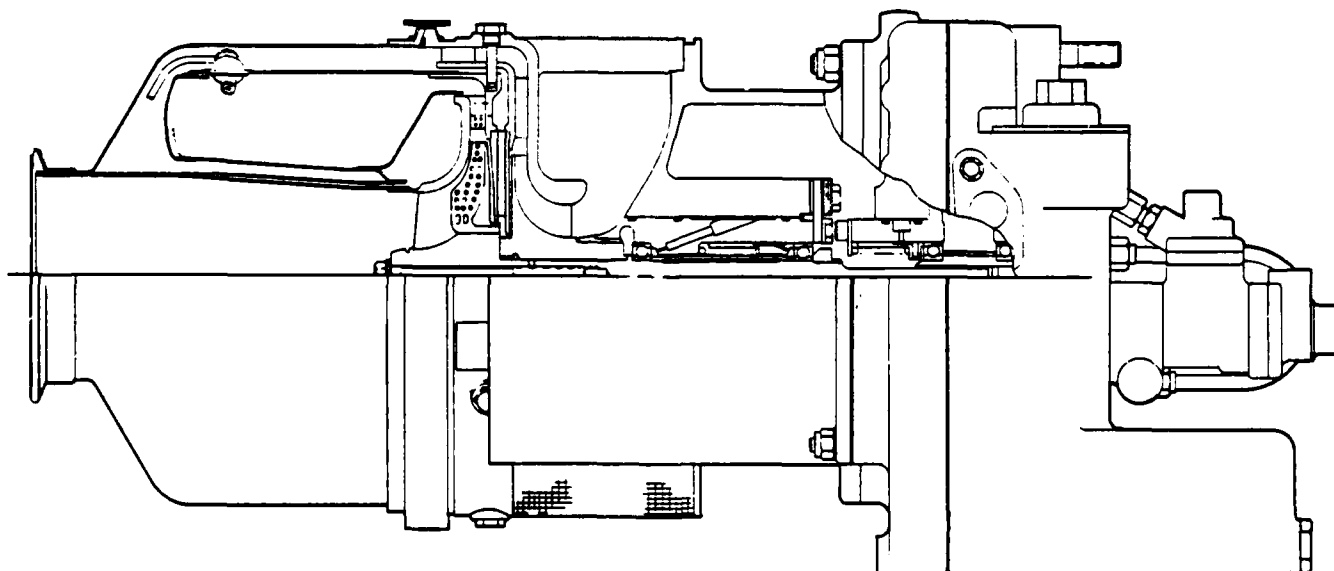


Figure 2-14. 40-kW Gas Turbine with Internally-Cooled Turbine Wheel

air is metered down the compressor/turbine seal plate to the hub of the MTR for passage through the rotor cavity and ejection at the tip. Nozzle cooling is also indicated as would be necessary for operation at a rotor inlet temperature of 2200°F.

## 2.7 MTR MONOROTOR

The monorotor (Ref. 3) possesses manufacturing and cost advantages in exchange for high thermal stresses originating from a pronounced axial (rather than radial) temperature gradient. The axial gradient is a function of the design pressure ratio and turbine inlet temperature. A somewhat higher cycle pressure ratio than 4.4 could be desired at MTR and HTR temperature levels to reduce the axial temperature gradient. The preliminary monorotor configuration selected (Figure 2-15) was used to commence thermal and stress analysis.

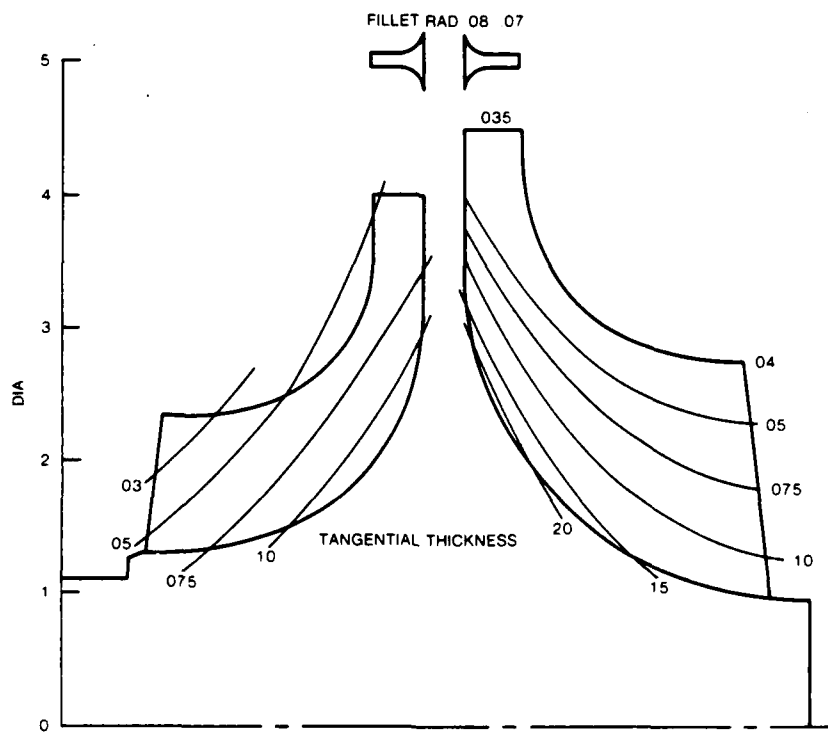


Figure 2-15. Monorotor Preliminary Configuration

### **2.7.1 Thermal and Stress Analysis of MTR Monorotor**

The monorotor configuration (Figure 2-15) was used to create a thermal nodal network for computation of the design point steady-state temperature distribution. Additional input to the internal flow data of Figure 2-11 were the tip seal leakage conditions shown in Figure 2-16 and the estimated compressor (side) air relative temperatures. The resulting temperature distribution for the monorotor is shown in Figure 2-17 and indicates a maximum localized temperature at the exducer tip of 1600°F. These data were used with a two-dimensional finite element stress model to determine dynamic and thermal stress loads.

Initial turbine blade stresses exceeded IN 792 material capabilities, and optimization of the blade taper ratios was conducted. The final selected rotor blade thickness variations are shown in Figure 2-18. Corresponding stresses are shown in Figure 2-19. Estimated stress rupture life for the life-limiting element was 300 hours. Disc burst overspeed was 143 percent. The burst mode would be tri-hub.

Compressor blade stresses shown in Figure 2-19 are centrifugal only and exclude out-of-radial plane bending stresses. Blade bending stresses were calculated separately and superposed on the centrifugal stresses to determine the net equivalent stress. The maximum equivalent blade stress, shown in Figure 2-19, was 122 ksi, with a corresponding metal temperature of 930°F. This stress level is conservative as the proximity of the disc and fillet would result in stress redistribution.

### **2.7.2 Application of MTR Monorotor**

A small 40-kW gas turbine, simple-cycle generator set powerhead incorporating an MTR monorotor is shown in Figure 2-20. The monorotor is inertia-welded to the rotor shaft to form a single-mass rotor system. Compressor discharge air is used to cool the turbine nozzles which are integrally cast with the compressor diffuser in a monostator assembly.

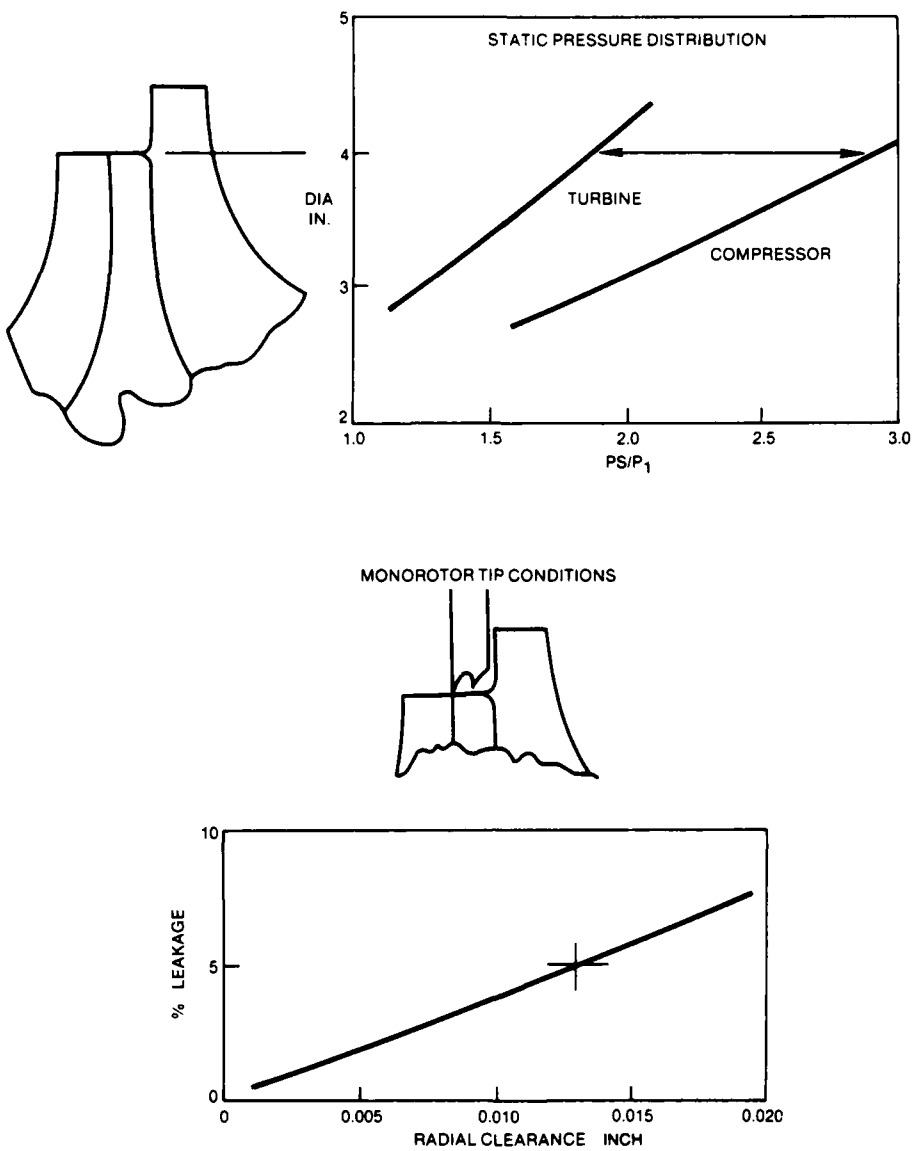


Figure 2-16. Monorotor Tip Conditions

## 2.8 MANUFACTURING COSTS

Preliminary drawings of the MRT internally-cooled design and monorotor (reference drawings 161260 and 161261) were provided to the casting vendor early in the program for manufacturing cost estimate purposes.

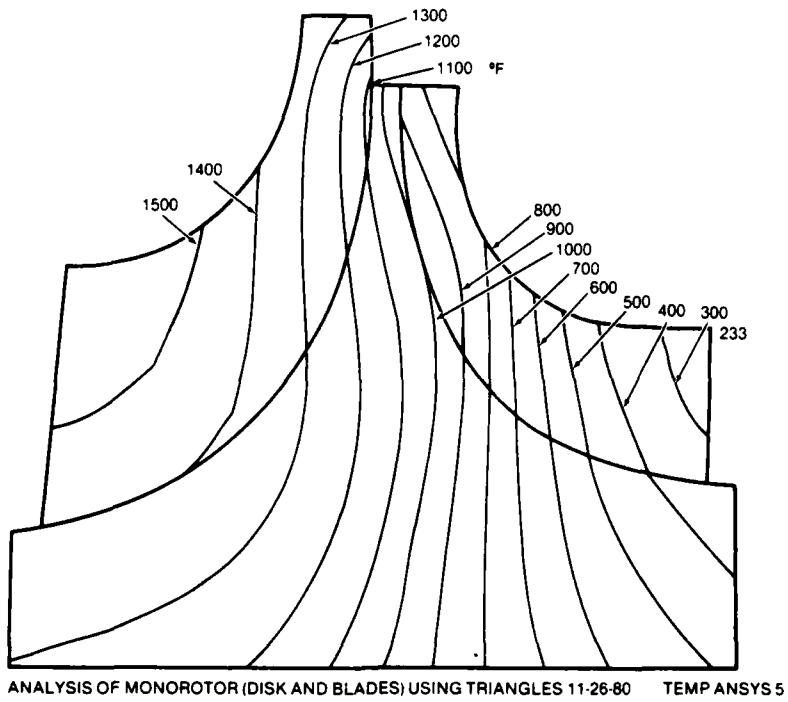


Figure 2-17. Monorotor Temperature Distribution

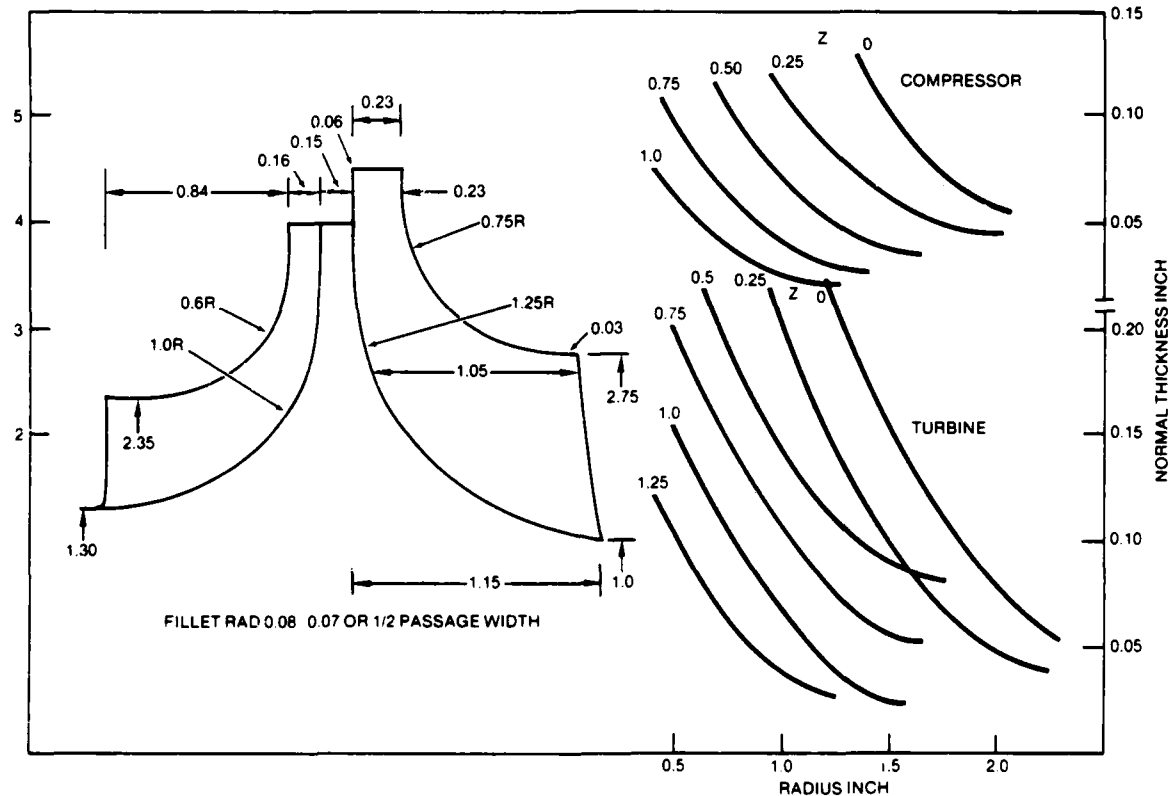


Figure 2-18. Final Monorotor Design

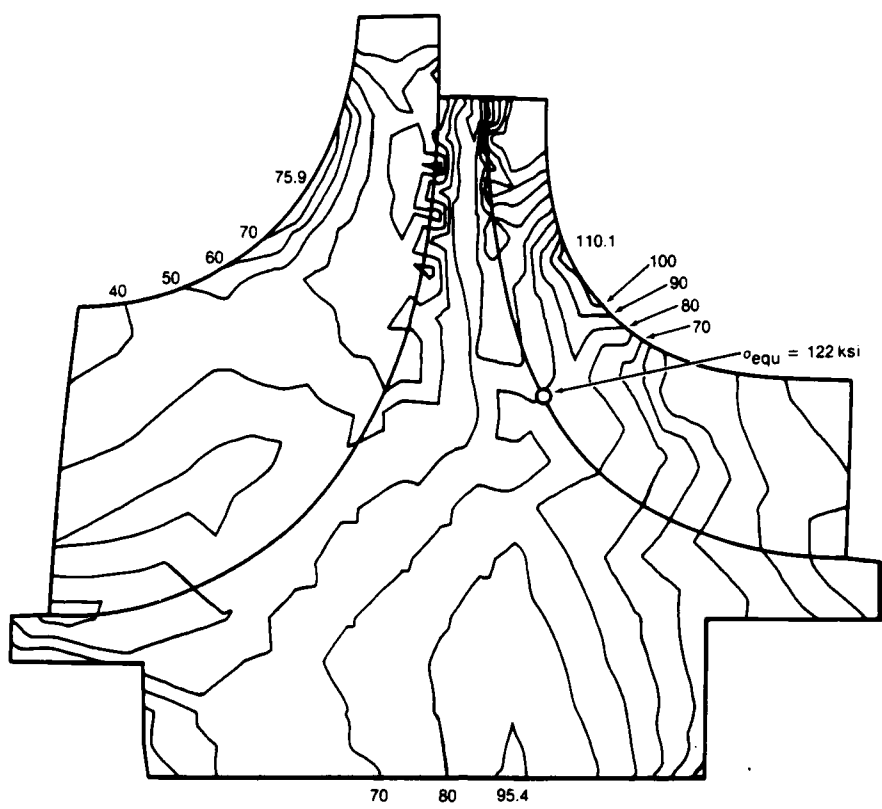


Figure 2-19. Monorotor Equivalent Stresses

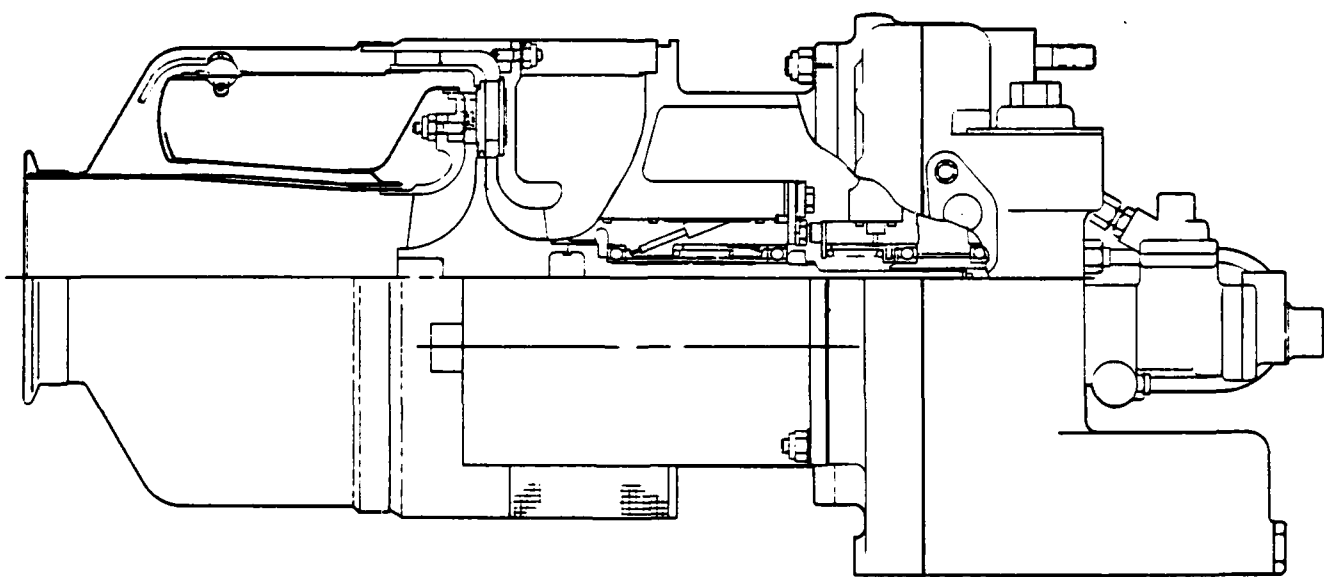


Figure 2-20. 40-kW Gas Turbine with Monorotor

A summary of quoted unit prices relative to the standard rotating assembly is listed in Table 2-6. The internally-cooled rotor would double the rotating assembly price and the monorotor would be half the price. The internally-cooled rotor differential price is within the cost goal of \$2000 to \$3000.

The significant cost advantage of the monorotor, together with its inertia-welded shaft and high durability, makes the configuration a prime candidate for the MTR application. The high temperature and low cost features can also be traded against superalloy material availability, in that an option exists to select lower grade superalloys for operation at current turbine inlet temperature loads in the lower range of 1700 to 1900°F.

## 2.9 SELECTION OF MTR CONFIGURATION

The results of Phase 1 MTR design studies are summarized in Table 2-7. Apart from stress rupture life, the monorotor possesses a clear advantage. The monorotor does not meet a stress rupture life requirement of 500 hours using IN 792 superalloy with a 25°F temperature and 15 percent stress margin. Using nominal stress/temperature and material strength levels, the monorotor stress rupture life would exceed 500 hours. On the basis of the data in Table 2-7, it was decided to select the monorotor for Phase I casting technology demonstration and mechanical integrity evaluation. (The finalized monorotor casting design is shown on drawing 161415.)

Table 2-6. Relative Costs of Rotating Assemblies

Assembly	Std. Cost	Internally Cooled Rotor	Monorotor
Compressor Rotor	1.0	1.0	1.17
Turbine Rotor	1.0	3.37	-
Shaft	0.28	0.28	0.17
Seal Plate	0.42	0.60	-
Bolt	0.07	0.07	-
Total	2.75	5.32	1.34
Percent Standard	100	193	48.7

Table 2-7. MTR Design Comparison

Design	Internally-Cooled Rotor	Monorotor
Burst Speed, %	129	143
Stress Rupture Life, hours	650	300
Relative Rotating Assembly Cost, \$	5.32	1.34
Durability	Poor	Good

## 2.10 MTR 30-KW REGENERATIVE GENERATOR SET

Following selection of the MTR monorotor, additional studies were completed on a 30-kW regenerative generator set meeting potential requirements for an advanced lightweight portable generator unit in the late 1980s.

The features of this 30-kW unit rated at 5000 feet, 107°F ambient temperature conditions, are shown in Figure 2-21. A single 12-inch diameter ceramic regenerator disc is aft-mounted on the engine centerline and is capable of attaining an effectiveness of 90 percent at design point conditions.

Estimated generator set performance is listed in Table 2-8, and operation at 2000°F with a pressure ratio of 4.4, a specific fuel consumption of 0.815 lb/kW-hr is projected equalling that of diesel generator sets.

## 2.11 HTR DESIGN

The HTR design will be constrained by:

- Turbine nozzle inlet gas temperature 2600°F
- Blade number 12 to 14
- Tip speed 2200 feet per second
- Fully machined rotor cost \$3000
- Ambient conditions 5000 feet, 107°F
- Stage efficiency (cycle) 80 percent
- Net cooling flow loss to cycle 3.0 percent
- Stress rupture life 600 hours
- Higher taper ratio, thicker blades

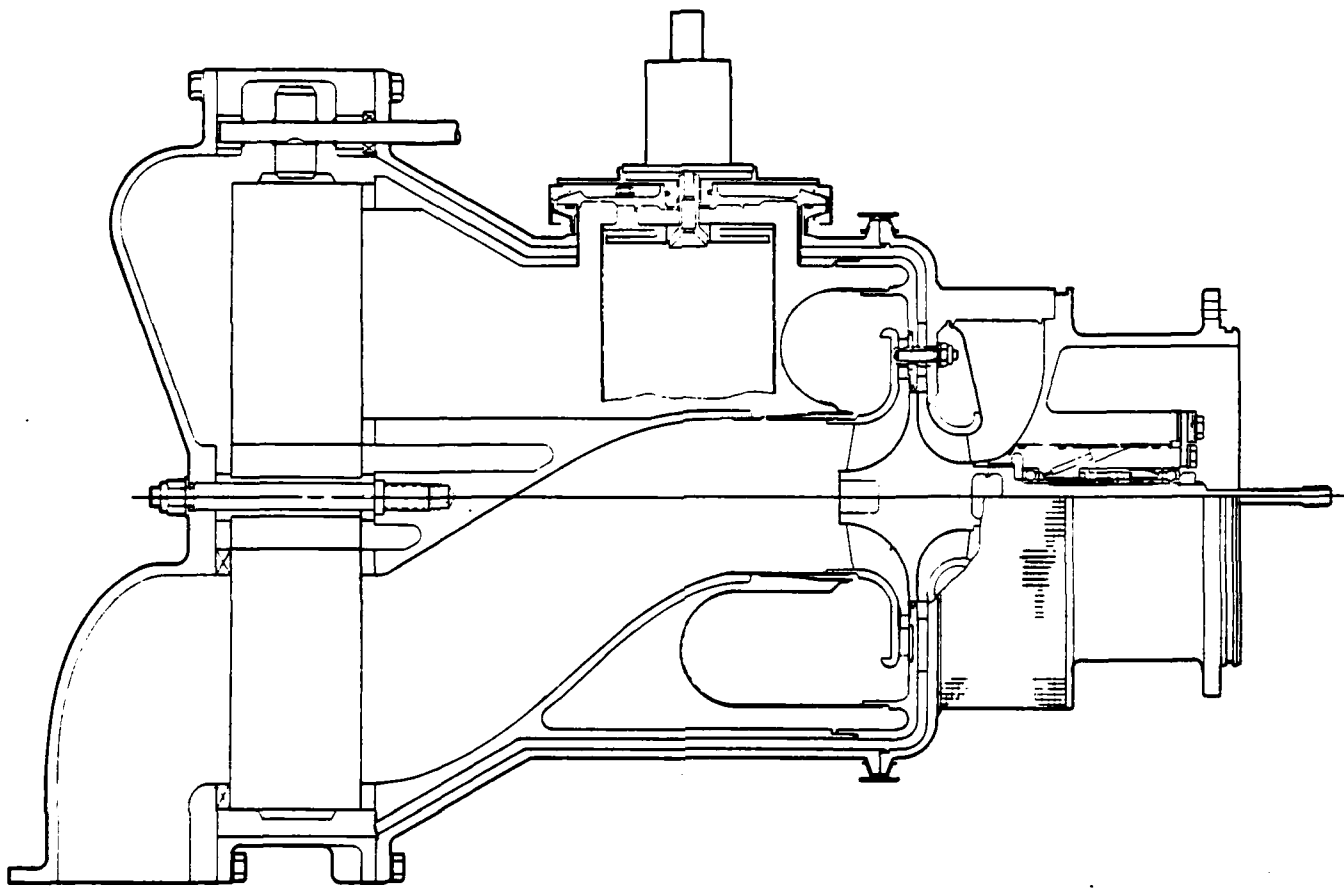


Figure 2-21. 30-kW Gas Turbine with 12-Inch Regenerator Disc

The cooling effectiveness required by a metal rotor would be about 0.50, necessitating a costly multi-pass internal cooling configuration with exducer trailing edge ejection. Temperature/tip speed combination and size are similar to that of a ceramic radial inflow turbine currently being developed under a DOE program (Ref. 2) with a design life goal of 100 hours at maximum temperature.

The HTR flow path selected (Table 2-9) was essentially that of the MTR with the tip diameter extended from 4.50 to 4.95 inches. This extended flow path was used to generate a two-dimensional finite element stress model.

Table 2-8. 30-kW MTR Regenerative Generator Set Performance\*

Parameter	Performance
Inlet Temperature Rise, °F	20
Rotational Speed, krpm	105
Compressor Pressure Ratio	4.4
Compressor Airflow, pps	0.58
Compressor Efficiency, %	76
Package Pressure Losses, %	3
Combustor Pressure Loss, %	5
Heat Exchanger Pressure Loss, %	4
Heat Exchanger Effectiveness	0.9
Turbine Nozzle Inlet Temperature, °F**	2200
Turbine Tip Speed, fps	2060
Turbine Velocity Ratio	0.63
Turbine Efficiency	0.825
Turbine Exit Temperature, °F	1565
Turbine Cooling Flow	5
Turbine Cooling Flow Equivalent Primary Loss, %	1.5
Regenerator Leakage, %	5.0
Gross Leakage (primary), %	6.5
Turbine/Compressor Flow, W/W <sub>c</sub>	0.95
Gross Shaft Power, hp	54.5
Mechanical Losses, hp	5.0
Net Output, hp	49.5
Combustor Efficiency, %	92
Generator Efficiency, %	85
Net Output, kW	31.4
Fuel Flow (Diesel), pph	25.6
SFC, lb/kW-hr	.815

\*5000 feet altitude, 107°F ambient temperature, 3% Pressure Losses, 10°F Inlet Heating

\*\*For design purposes, turbine nozzle inlet temperature is assumed equal to turbine rotor inlet temperature.

Stress results for a HTR-sintered silicone carbide turbine rotor with a flat-back disc contour showed excessively high stresses in the disc. Optimization of the backface contour was conducted to reduce these high stress levels by the addition of considerable backface slope. Figures 2-22 and 2-23 show estimated rotor temperature gradients and stresses. The probability of failure of this rotor was calculated from:

Table 2-9. HTR Design Point

Parameter	Design Point
Pressure Ratio	4.0
Rotational Speed, rpm	105,000
Airflow, pps	0.58
Nozzle Inlet Temperature, °F	2600
Flow Function, $w\sqrt{T/P}$ , inlet	0.50
Efficiency (Total-Static), %	81
Tip Diameter, inch	4.95
Tip Speed, fps	2260
Tip Width, inch	0.22
Shroud Clearance, inch	0.035
Number of Blades	12
Exducer Shroud Diameter, inch	2.75
Exducer Hub Diameter, inch	0.9
Exducer Blade Thickness (RMS), inch	0.035
Exducer Blade Angle (RMS), degree	56
Velocity Ratio	0.63
Tip Incidence, degree	33.0
Blade Tip Relative Temperature, °F	2230
Exhaust Gas Temperature, °F	1903

$$P = 1 - e \left[ \frac{1}{-V_0} \sum \left( \frac{\sigma}{\sigma_0} \right)^M \Delta V \right]$$

where:  $V_0 = 0.010 \text{ in.}^3$

$\sigma$  = sample stress volume

$\sigma_0 = 58.3 \text{ ksi}$

$M = 10.21$

For the hub and blades, the probability of failure was 94 and 4.3 percent respectively. For the blades and hub combined, the failure probability was 94.6 percent.

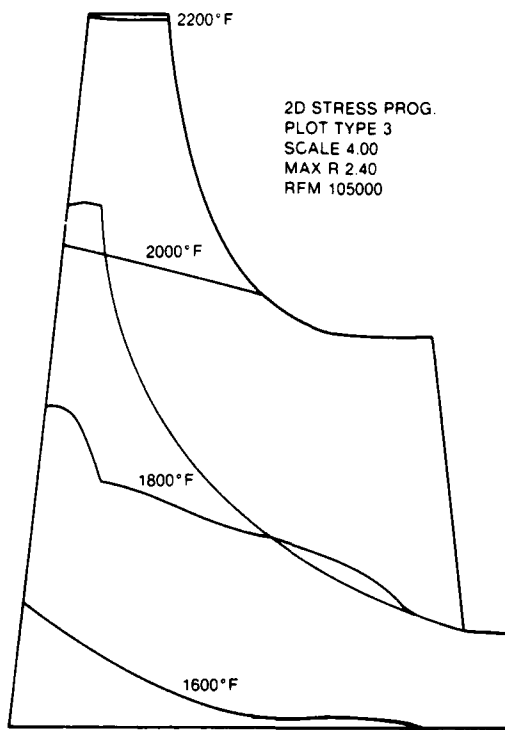


Figure 2-22. HTR Rotor Temperatures

The high failure probability questions the feasibility of the HTR ceramic approach. Options to lower stresses would be reduction of rotational speed or tip diameter with subsequent performance penalties.

With further optimization and reduction in tip speed, the 40 ksi maximum stress region could be eliminated, and the failure probability would improve to 13.9 percent.

## 2.12 PHASE I DESIGN SUMMARY

Two mid-temperature 4.50-inch tip diameter radial inflow turbine rotors were designed for a maximum turbine nozzle inlet temperature of 2200°F, representative of the threshold for simply-cooled metallic technology. Rotational speeds for both rotors were 105,000 rpm. One rotor was internally air-cooled and the other conduction-cooled in a monorotor arrangement.

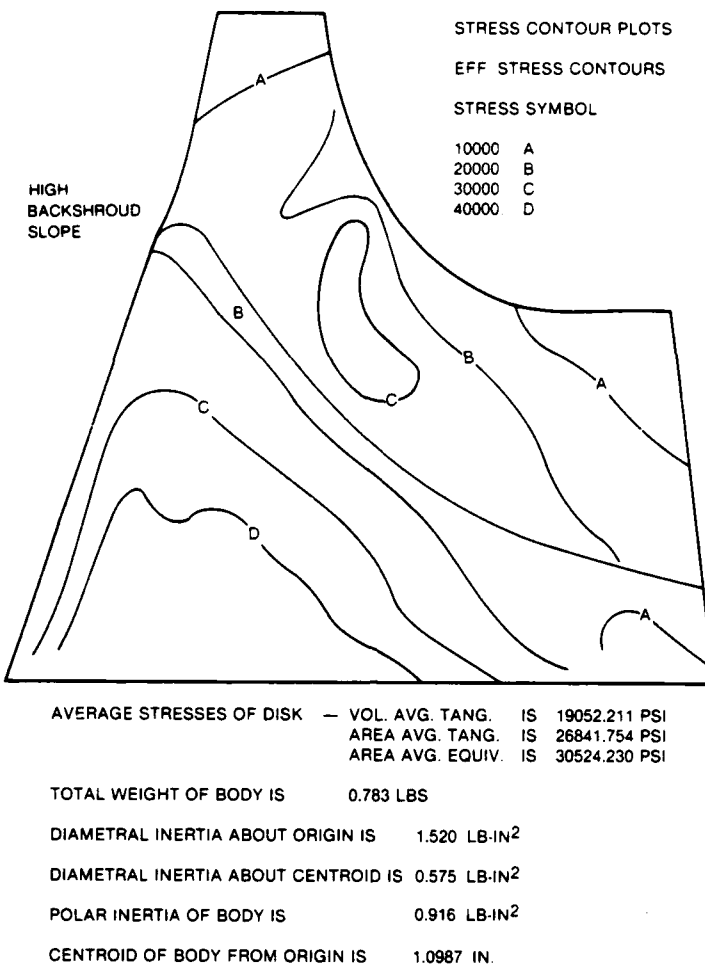


Figure 2-23. HTR Rotor Stresses

Detailed aerothermodynamic, structural, and cost analyses of both rotors revealed slightly lower stress rupture life but improved burst speed margin and significantly lower manufacturing costs for the monorotor configuration.

Technology application studies of highly portable, lightweight, ground power gas turbine generator sets showed that significant improvements to the power-to-weight ratio were possible. In combination with exhaust heat recovery with a ceramic regenerator, the MTR turbine had the potential of a highly thermal-efficient 30-kW generator set equal to that of the diesel engine.

Design studies were extended to a ceramic high temperature rotor operating at a maximum turbine nozzle inlet temperature of 2600°F. Using sintered silicone carbide material, it was determined that rotor failure probability was unacceptable and that the relatively small performance benefit, which occurred when operating temperature was increased from the MTR to the HTR configuration, questions the viability of this concept.

As a result of Phase I studies, it was recommended that the MTR monorotor be selected for casting technology demonstration and structural integrity evaluation. The casting tooling and three monorotors cast in IN 792 material, satisfying drawing 161415 dimensional and material specification requirements, were recommended for procurement. It was further recommended that a shaft compatible with the current T-20G bearing system be inertia-welded to one machined monorotor casting for spin pit structural integrity evaluation.

### 3.0 PHASE II FABRICATION

An approval of the Phase I Design Analysis, procurement of monorotor tooling and castings from Howmet Corporation was initiated.

#### 3.1 MONOROTOR CASTINGS

Five monorotor castings, in hipped IN 792 material with X-rays and chemical report, were received on January 6, 1982. Figure 3-1 shows three views of the casting. Preliminary physical inspection showed that the blade geometry meets the design drawing requirements. The chemical report is attached in Appendix A. Two rotors were destructively tested at Howmet to determine material properties, and grain structure (Table 3-1). Etching results are shown in Figure 3-2 and indicate an acceptable grain pattern.

Table 3-1. Monorotor Material Properties

Casting	A 004		A 003	
	1 Bar	2 Bar	1 Bar	2 Bar
Room Temperature UTS (ksi)	163	159	163	169
<b>Properties</b>				
Yield (ksi)	134	135	141	124
Elong %	7.5	7.2	6.3	8.7
R/A %	8.6	8.5	7.8	8.6
<b>Stress Rupture</b>				
1400°F at 94 ksi, hrs	106	---	105	---
1700°F at 39 ksi, hrs	---	72	---	72
Elong %	7.5	10.1	4.7	8.9
R/A %	6.2	16.7	10.9	13.3

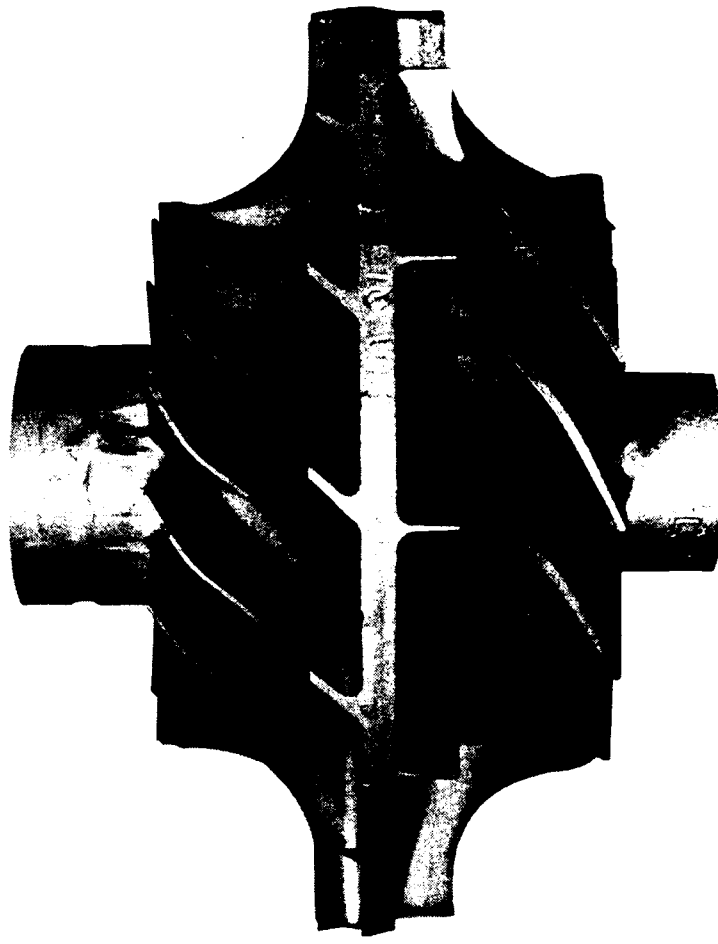


Figure 3-1. Monorotor Casting

### 3.2 INERTIA WELDED SHAFT

Prior to inertia welding of the shaft proper, sample welding was conducted using specimens of the shaft and monorotor materials to optimize the welding process. Tests of segments from the welds indicated that a 100 percent bend was not possible, confirming the subcontractor's experience that up to 70 percent weld was feasible. Since torsional strength calculations revealed that a 100 percent weld would provide a margin of safety of 558 percent, it was decided to accept the manufacturer's procedure.

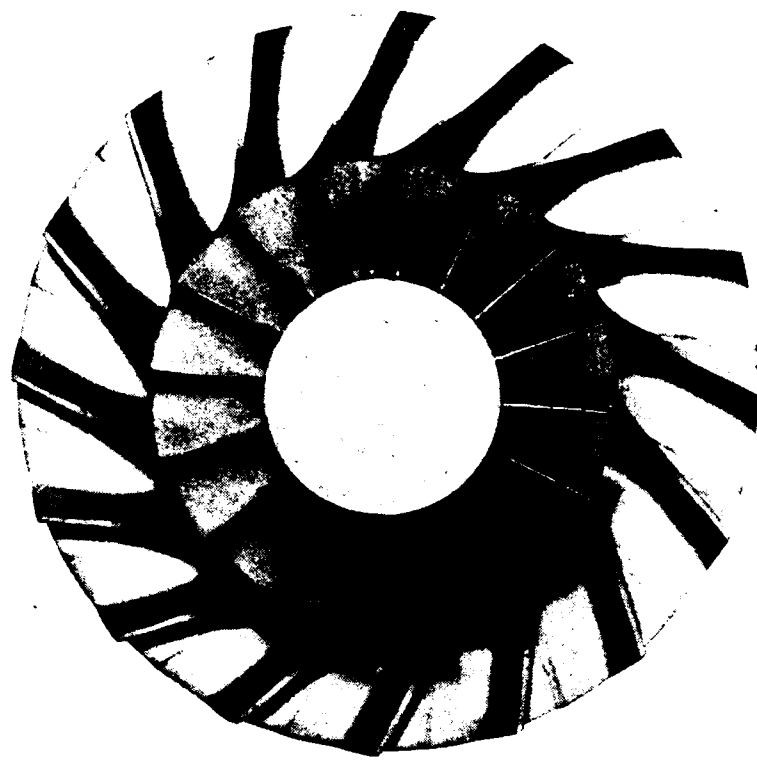


Figure 3-1. Monorotor Casting, Contd

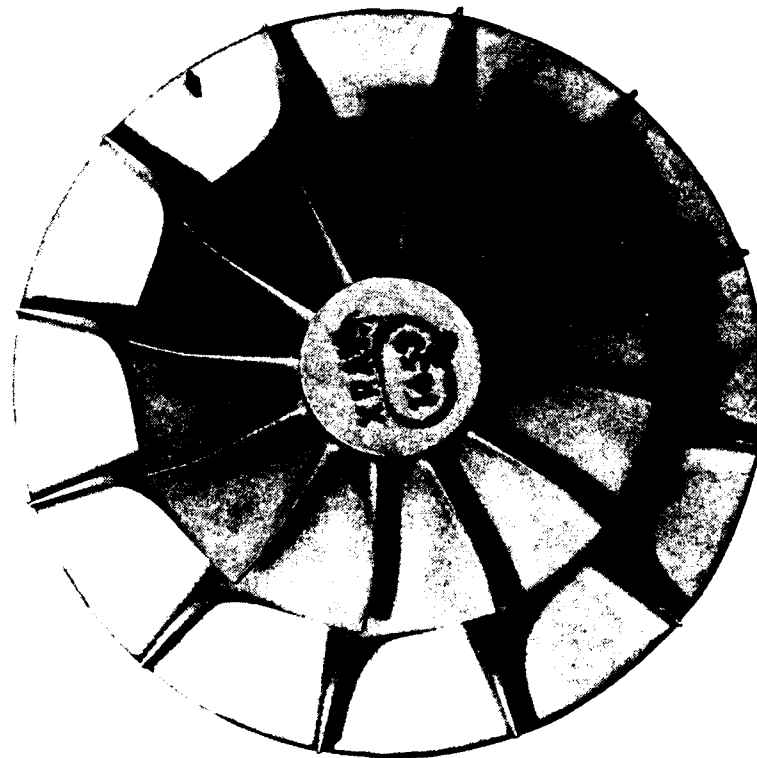


Figure 3-1. Monorotor Casting, Contd

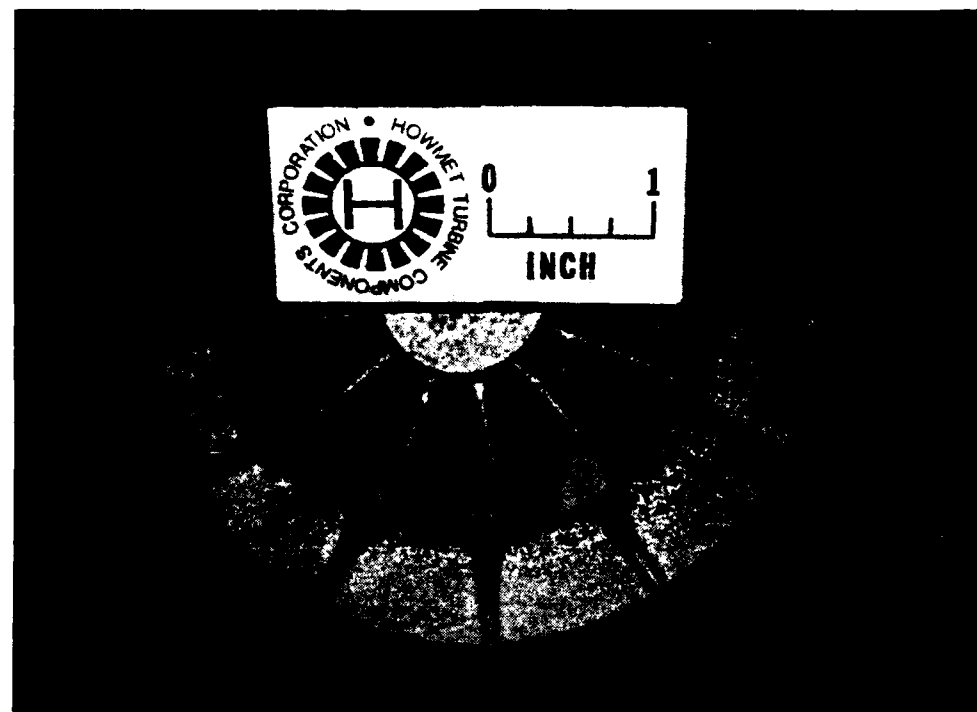


Figure 3-2. Etching Results

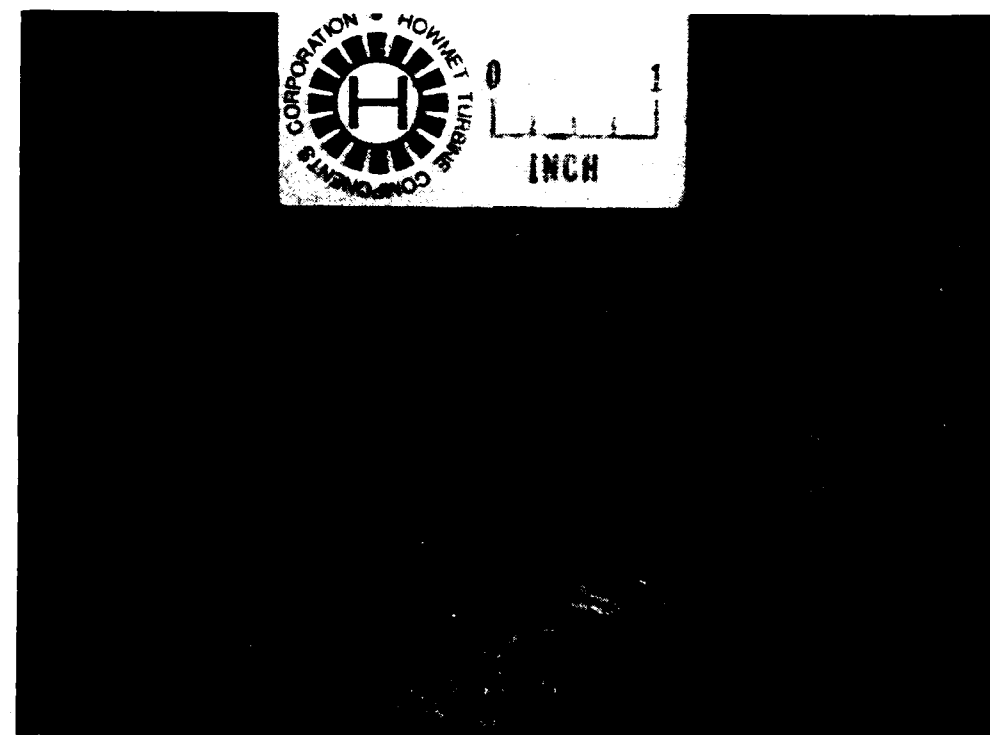


Figure 3-2. Etching Results, Contd

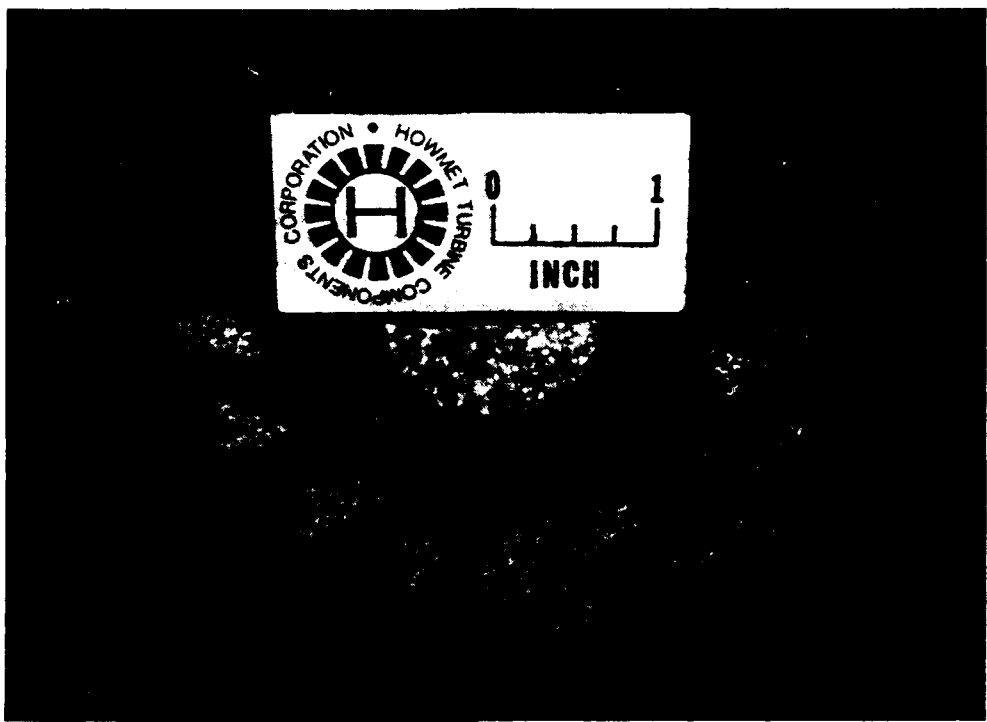


Figure 3-2. Etching Results, Contd

The completed monorotor and shaft is shown in Figure 3-3 prior to holographic testing and assembly in the bearing cartridge for balancing.

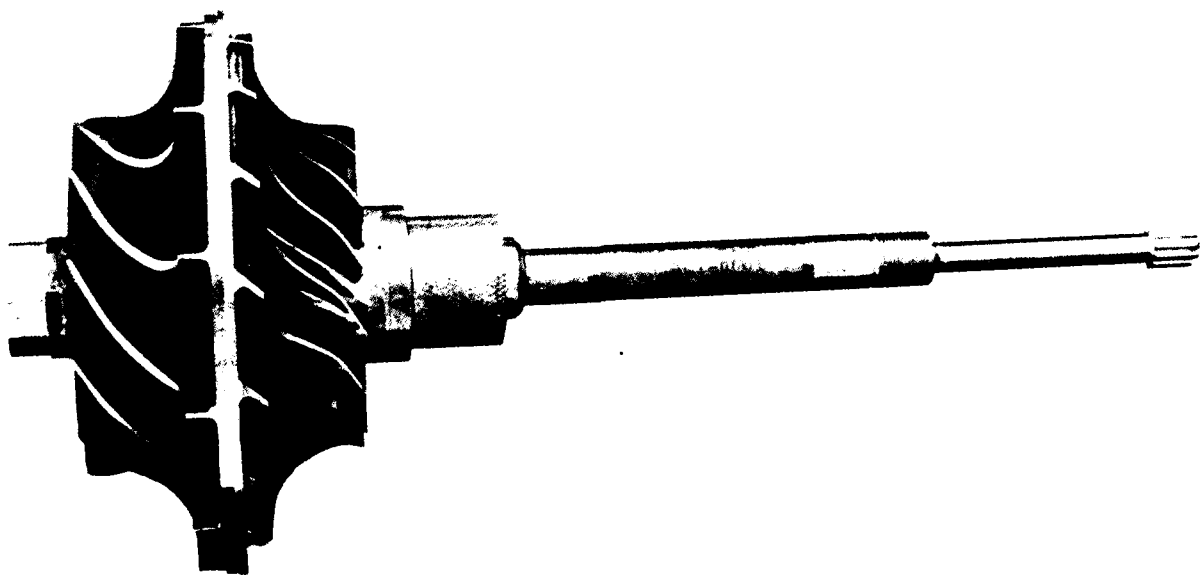


Figure 3-3. Completed Monorotor and Shaft

### 3.3 HOLOGRAPHIC TESTING

The holographic test set-up is shown in Figure 3-4. Figures 3-5 and 3-6 show the first fundamental compressor inducer and turbine exducer frequency patterns, respectively. Frequency testing was conducted on the casting before and after machining, as indicated below:

Frequency	Compressor	Turbine
Acoustic - before machining, Hz	7475	8400
Holographic - after machining, Hz	8475	9300

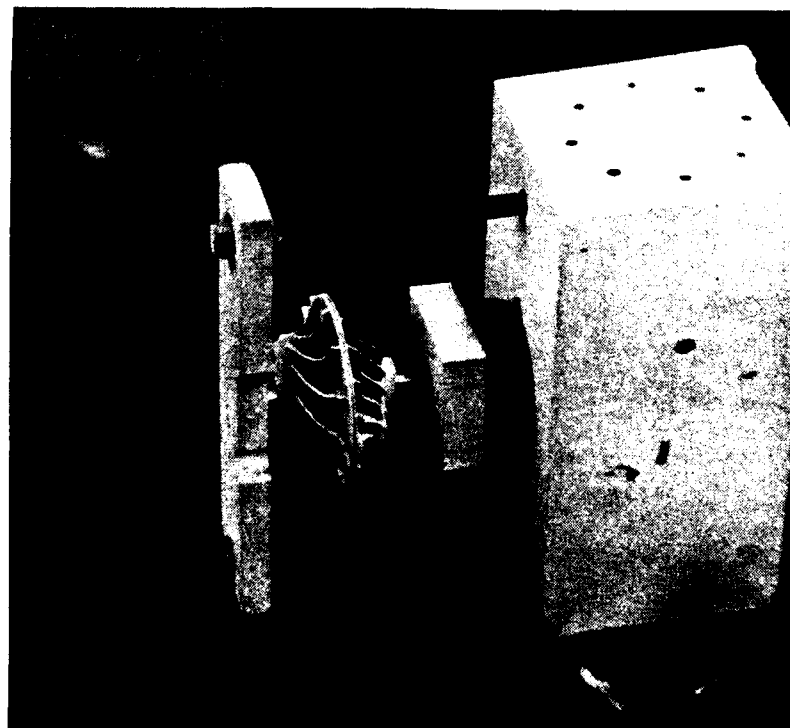


Figure 3-4. Holographic Test Set-Up



Figure 3-5. Compressor Inducer Frequency Pattern



Figure 3-6. Turbine Exducer Frequency Pattern

### 3.4 BALANCING

Initial balance checks revealed that excessive material removal would be necessary to achieve a force balance, in that the rotor was out of balance by 0.236 in.-oz. Examination of the drawing requirements showed that with normal casting tolerances and permissible machinery eccentricities, a part could be out of balance by as much as 0.518 in.-oz. As drawing permissible material removal areas were insufficient to attain such a balance, an alternate method was proposed. Figure 3-7 shows revised areas where material removal is permitted. Removing a maximum of 0.070 in. deep material in three places is sufficient to balance the rotor in the worst case. The compromise is reduced sealing capability of the tip labyrinth seal. An alternate solution in high quantity production would be to implement a rotor machining technique, whereby the bearing race diameters are on the same axis as the center of mass of the rotor. A suggested means of accomplishing such a technique is described in Appendix B.

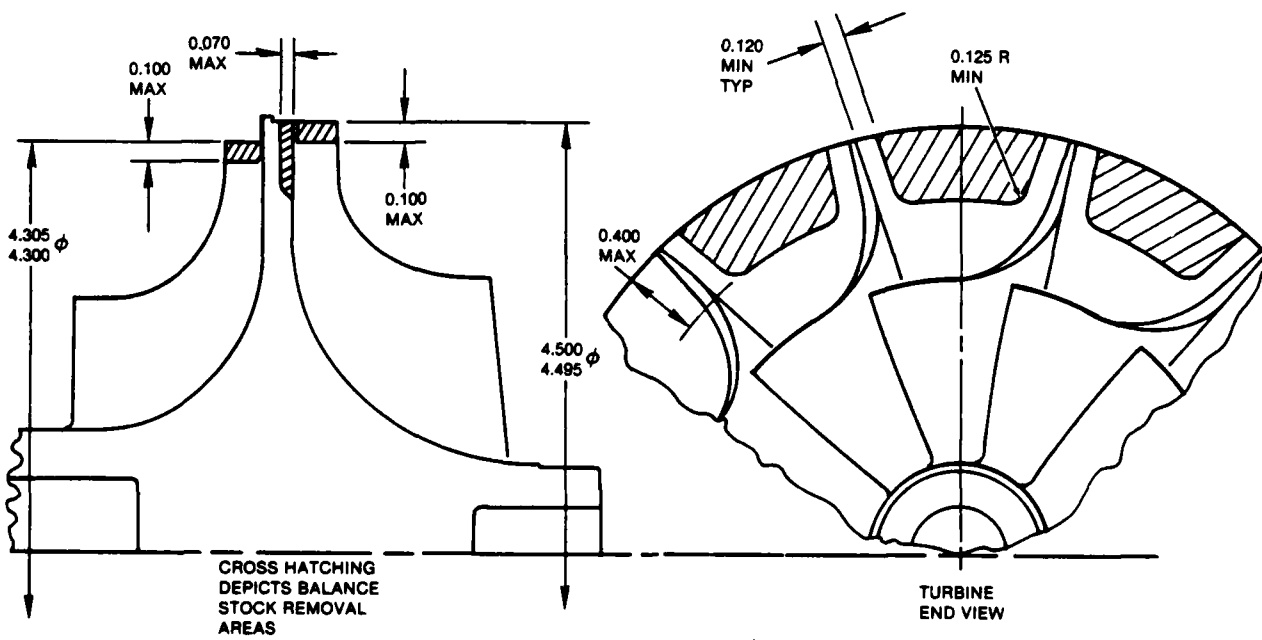


Figure 3-7. Areas of Material Removal

### 3.5 SPIN TESTING

The stress coated monorotor and spin fixture were mounted vertically in the high speed spin pit facility and initial check out runs were made to identify the first critical speed, which was observed close to 14,000 rpm. The fixture was subsequently extracted from the pit for examination and showed no evidence of stress coat cracking. A second acceleration was made to 20 percent and then 25 percent design speed where spalling of the stress coat was observed. Apparently the stress coat had not been applied uniformly, resulting in the spalling (Figure 3-8) rather than discrete cracking.

A third acceleration was made up to 98,000 rpm prior to the speed falling off and the operator discontinuing the test. Post examination showed that the forward bearing had apparently failed on shutdown.

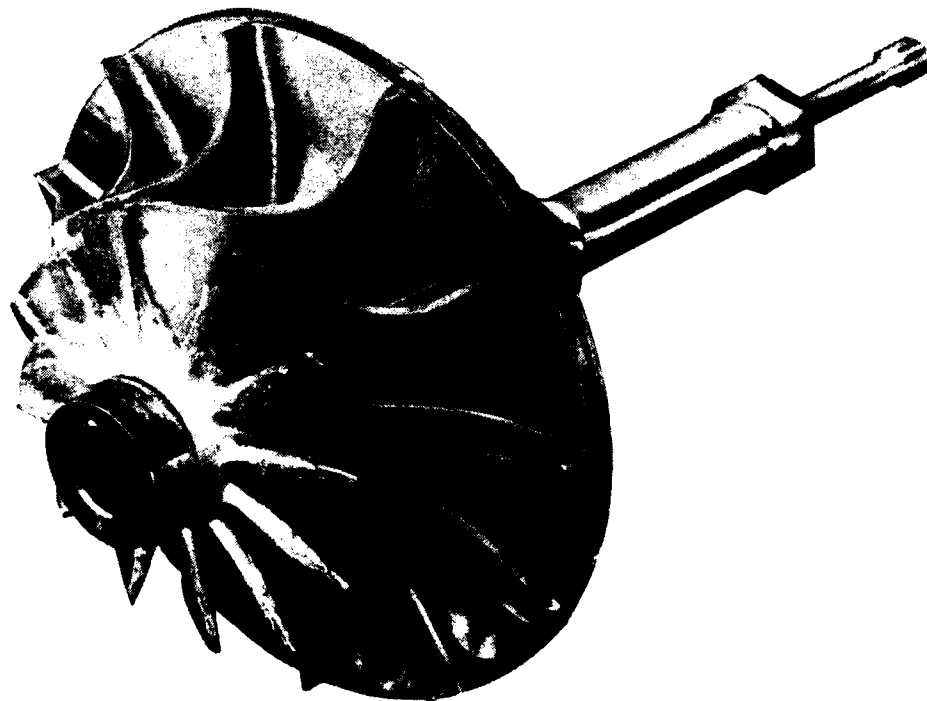


Figure 3-8. Monorotor Stress Coat Spalling

Previous difficulties had been experienced with a similar dynamic assembly with instability of the 0.125 inch diameter drive shaft from the spin head to the rotor near 100,000 rpm. Accordingly, it was decided to stabilize the drive shaft extension by incorporating the engine high speed pinion bearings. (See Figure 3-9.)

The modified spin fixture is shown in Figure 3-10 as mounted in the spin pit. Initial checkout revealed that excessive oil-flow churning and bearing preload prevented reaching design speed. The churning and preload were reduced, making it possible to reach 120 percent design speed with a spin head turbine inlet pressure of 180 psig. Subsequently, several spin tests were made measuring speed, time, and proximity probe displacement at the exducer hub. Figure 3-11 shows a maximum displacement of 1.7 mil at the critical speed of 13,700 rpm. The monorotor tip diameter was measured before and after spinning. Permanent growth was recorded as follows:

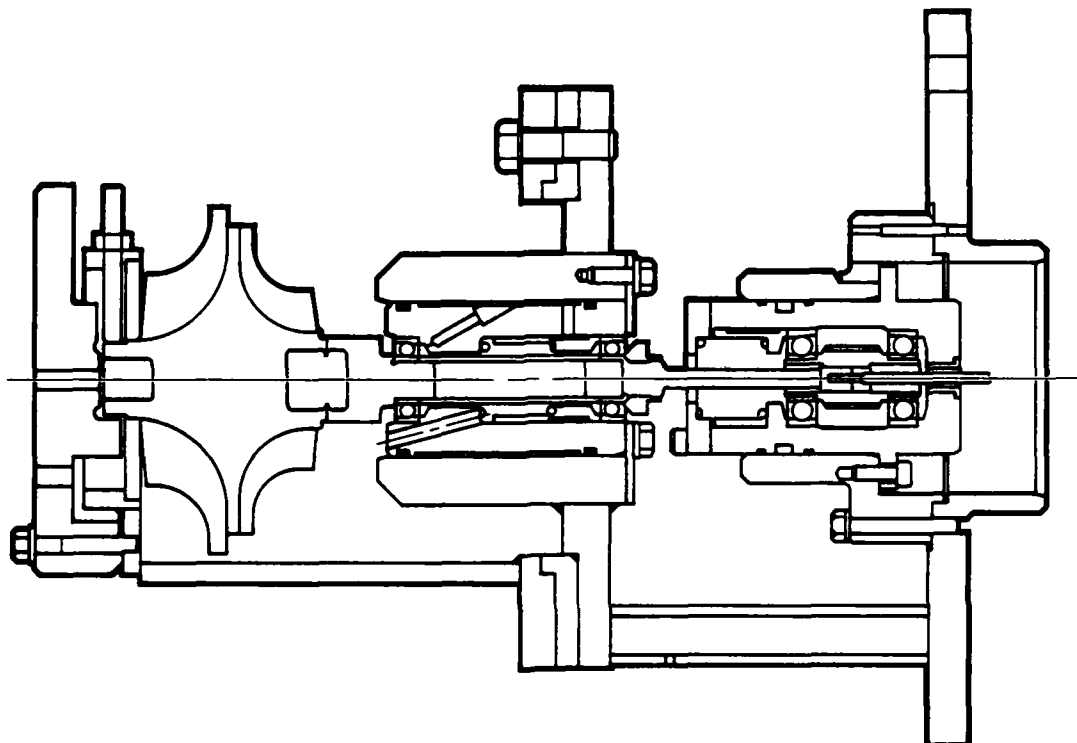


Figure 3-9. Modified Spin Fixture

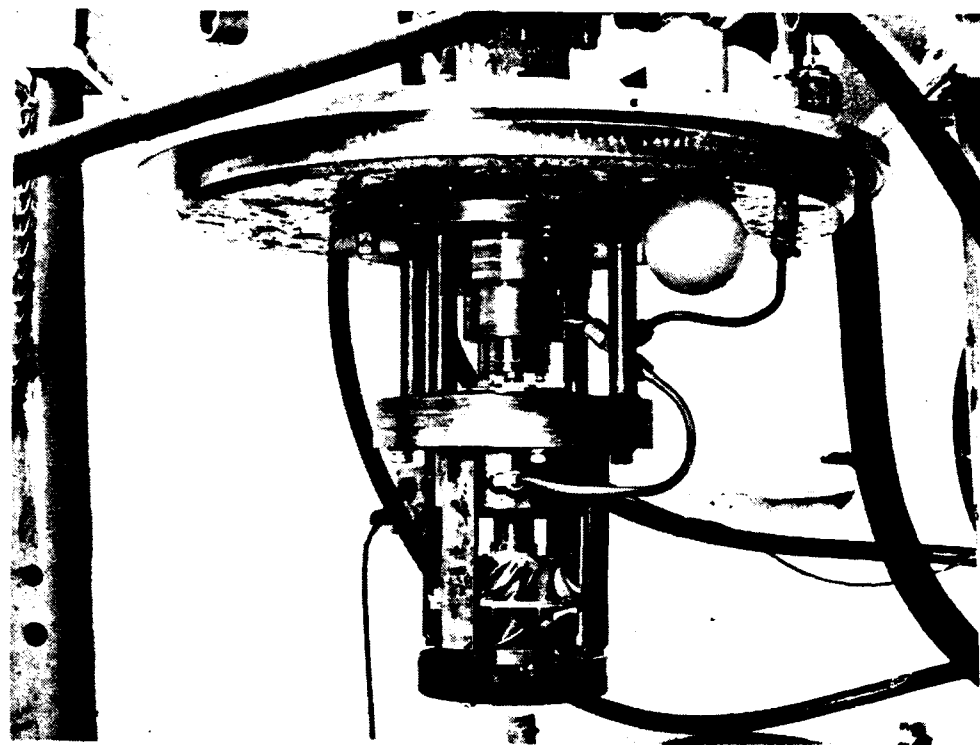


Figure 3-10. Vertical Spin Pit

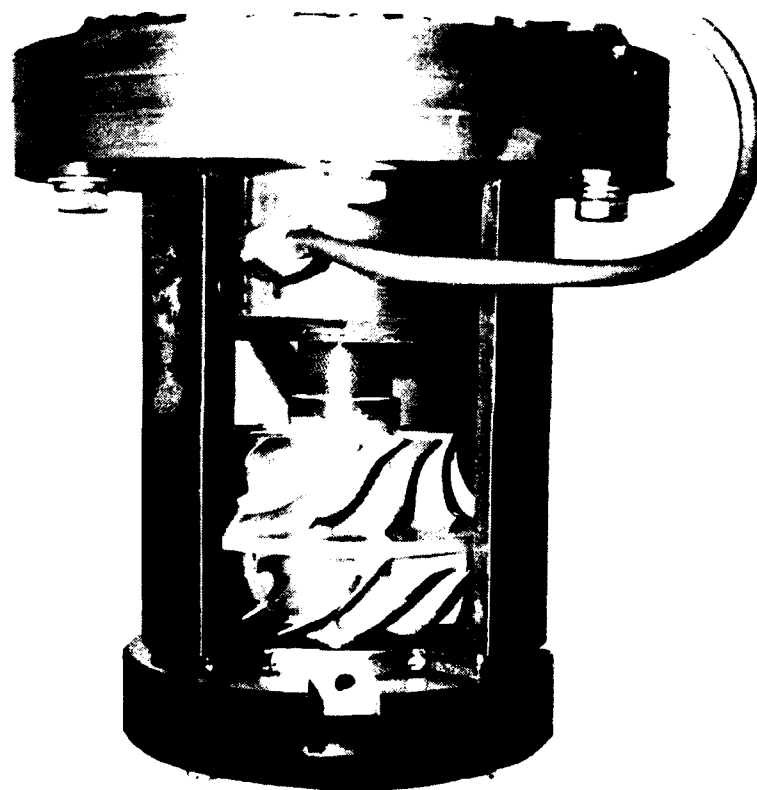


Figure 3-10. Vertical Spin Pit, Contd

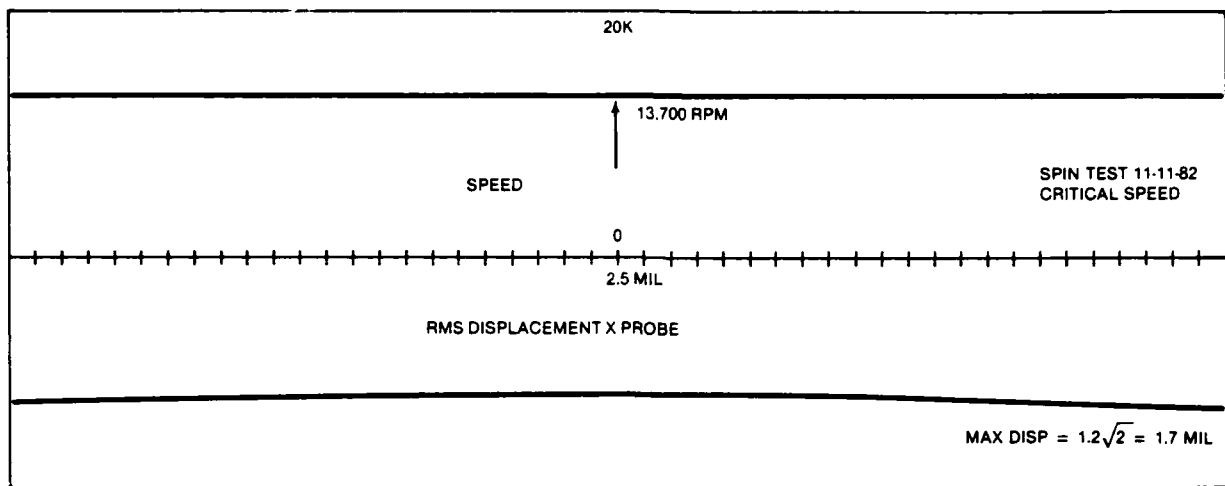


Figure 3-11. Spin Test Measurement

Speed, rpm	Tip Diameter Permanent Growth, inch
98,000	0.000
124,000	0.003
126,000	0.0035
130,000	0.0105

As per item 8 of the test agenda, a final spin run was made to 135,000 rpm where a burst was accomplished. The type of burst was a desirable, minimum energy rim fragmentation, as illustrated in Figure 3-12.

The resulting imbalance forces sheared the shaft in two places, one ahead of the aft bearing race, and one at the inertia weld, as illustrated in Figure 3-13.

The test monorotor was slightly different from the original design in that the disc extended completely to the turbine tip, 4.5 inch diameter, and thus had both increased disc weight and stress. Extension of the disc was implemented to facilitate eventual assembly with the turbine nozzle.

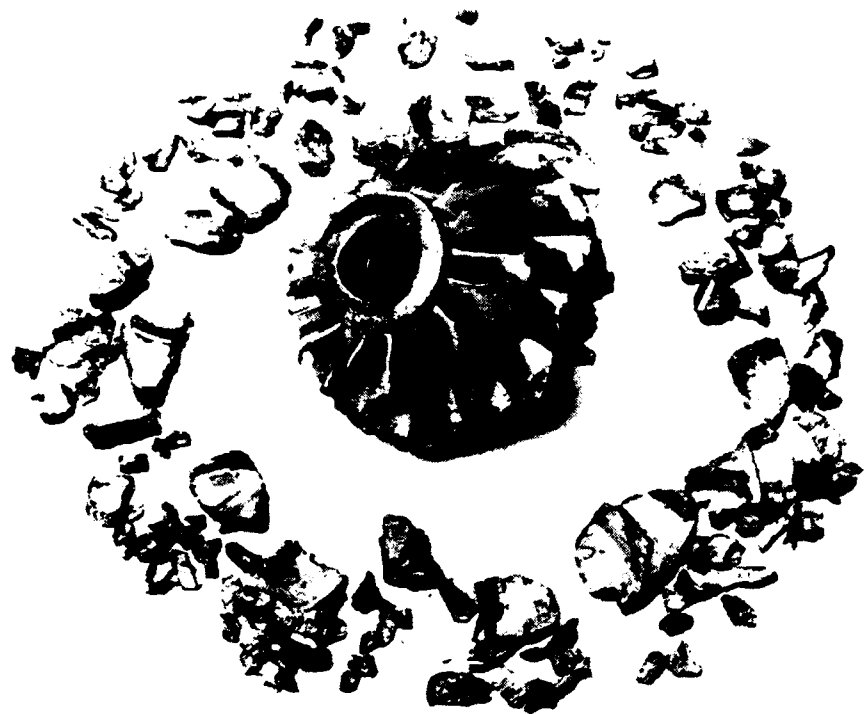


Figure 3-12. Rim Fragmentation

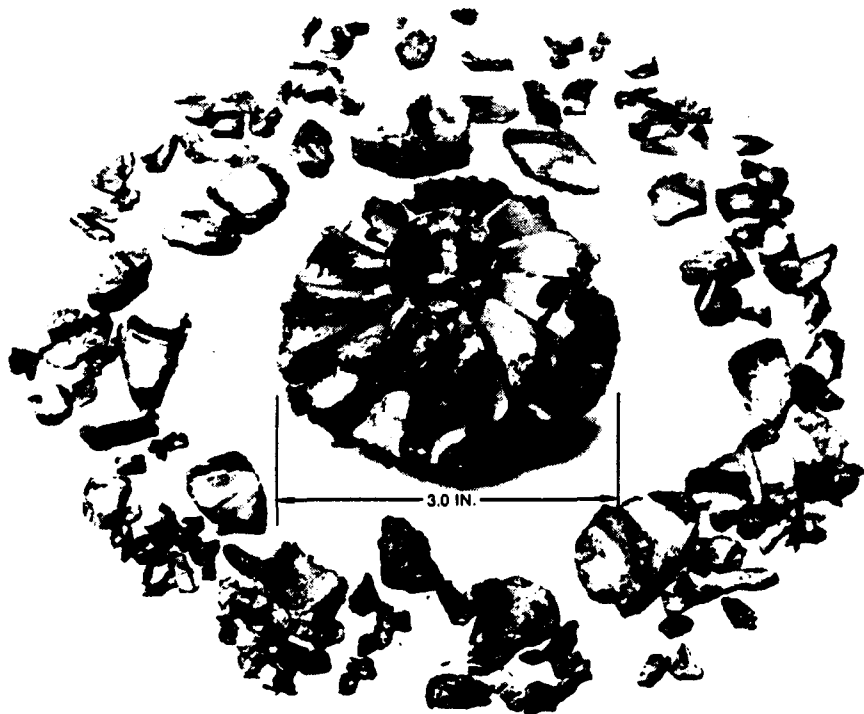


Figure 3-12. Rim Fragmentation, Contd

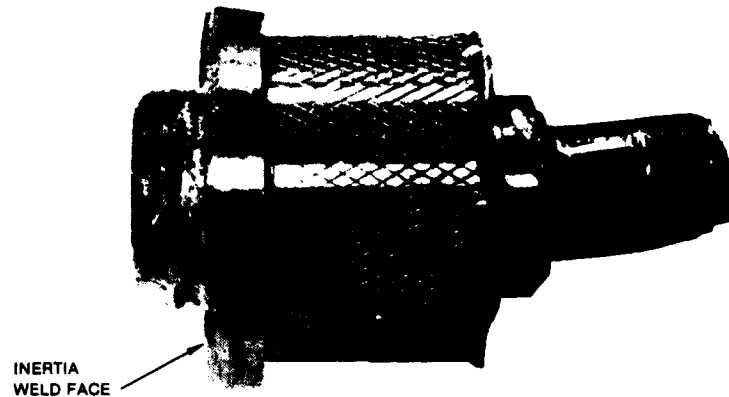


Figure 3-13. Shaft Shearing Due to Imbalance Forces

Comparative maximum disc tangential stresses and burst speeds estimated from the finite element stress model for the two configurations are listed below using the material tested U.T.S. of 164 ksi.

Configuration	Original Design	Extended Disc
Blade Weight, lb	0.54	0.54
Disc Weight, lb	1.89	1.99
Maximum Tangential Stress, ksi	64.2	69.8
Radial Stress, ksi	84	103
Burst Margin on Radial Stress, %	140	127

Test Burst Margin = 128.5%

Rim fragmentation occurred at a mean diameter of 3.0 inches, which corresponds to the position of maximum radial stress.

The predicted and actual burst speeds agree, presuming radial overstress was the mode of failure. Thus, disc contouring has been demonstrated to be an important monorotor design aspect.

### 3.6 SUMMARY OF PHASE II TESTS

- Successful mechanical integrity testing was completed as per approved test agenda.
- A disc burst was demonstrated in a desirable minimum energy rim fragmentation mode
- The disc burst was caused by radial stresses exceeding the material limits.
- Balancing of the monorotor is a potential manufacturing problem. Methods of machining should be investigated to permit location of the machining center on the center of mass.
- Fixture spin testing should be conducted with the minimum possible amount of bearing oil flow.
- The drive shaft sheared in two places, indicating the inertia-welded joint may only be as strong as the smaller shaft. It is recommended that the weld joint be metallurgically examined.

#### 4.0 CONCLUSIONS AND RECOMMENDATIONS

Two mid-temperature 4.50-inch tip diameter radial inflow turbine rotors were designed for a maximum turbine nozzle inlet temperature of 2200°F, representative of the threshold for simply-cooled metallic technology. Rotational speeds for both rotors were 105,000 rpm. One rotor was internally air-cooled and the other conduction-cooled in a monorotor arrangement. Detailed aerothermodynamic, structural, and cost analyses of both rotors revealed slightly lower stress rupture life but improved burst speed margin and significantly lower manufacturing costs for the monorotor configuration.

Technology application studies for highly portable, lightweight, ground power gas turbine generator sets showed that significant improvements to the power-to-weight ratio were possible. In combination with exhaust heat recovery with a ceramic regenerator, the MTR turbine had the potential of a highly thermal-efficient 30-kW generator set equal to that of the diesel engine.

Design studies were extended to a ceramic high temperature rotor operating at a maximum turbine nozzle inlet temperature of 2600°F. Using sintered silicone carbide material, it was determined that rotor failure probability was unacceptable and that the relatively small performance benefit, which occurred when operating temperature was increased from the MTR to the HTR configuration, questions the viability of this concept .

As a result of Phase I design studies, monorotor casting tooling and five monorotor castings in hipped IN 792 superalloy were procured. One casting was machined and inertia welded to an existing T-20G shaft, to form a single-mass rotating assembly. The rotating assembly was mounted to an existing T-20G bearing capsule for mechanical testing in the high speed spin pit facility. Spin testing was comprised of three runs to 120 percent design speed and a burst demonstration. The burst occurred at 128.5 percent design speed and was of the rim fragmentation type.

The development effort to date indicates that the monorotor is a practical approach to low cost, high temperature, small gas turbine generator sets of the 30-kW size, and continuation of the program into an Aerodynamic Design Verification Phase (in Appendix B) is recommended. Two minor problems require further resolution and involve an improved balancing technique for the monorotor and additional development of the inertia welding process to improve weld joint strength.

## 5.0 REFERENCES

1. Branger, M., "Veil Cooling of Radial Flow Turbines," Final Report prepared by AiResearch Manufacturing Co., for the Office of Naval Research, October 1963.
2. Calvert, G.S. and Okapu, U., "Design and Evaluation of High Temperature Radial Turbine," USAAVLABS Technical Report 68-69, January 1969.
3. Rodgers, C., "Advanced Radial Inflow Turbine Rotor Program - Design and Dynamic Testing," NASA CR-135080, and Solar ER 2519.
4. Hamed, M., Baskharone, E. and Tabakoff, W., "A Numerical Study of the Temperature Field in a Cooled Radial Turbine Rotor," NASA CR-13795.
5. B.A. Ewing, D.S. Monson, "U.S. Army/DDA High Temperature Radial Turbine," AIAA-80-0301.
6. R.A. Johnson, "Conceptional Design Study of an Improved Gas Turbine (IGT) Powertrain," NASA CR-159604.
7. Engineering Staffs of Ford Motor Co. and AiResearch Co., " Conceptional Design Study of Improved Automotive Gas Turbine Powertrain," - Final Report NASA TR-159580.

**APPENDIX A**

**CERTIFIED REPORT OF CHEMICAL ANALYSIS AND MECHANICAL TESTS**

**HOWMET TURBINE COMPONENTS CORPORATION**  
**AUSTENAL LA PORTE DIVISION**  
 1110 EAST LINCOLNWAY, LA PORTE, INDIANA 46350

Solar Turbines International  
 2200 Pacific Highway  
 San Diego, CA 92138

DATE  
 12/11/81

**CERTIFIED REPORT OF CHEMICAL ANALYSIS AND MECHANICAL TESTS**

OR PART NO.	PURCHASE ORDER NO.	QUANTITY SHIPPED	SPECIFICATION NO.
1415	1653-30427-Y48	2	77-0502
	DATE SHIPPED	INVOICE NO.	ALLOY
	12/11/81	124729	IN782 Mod 5A

CHEMICAL ANALYSIS												
FOR NO.	NO. OF Pcs	C	Si	Mn	Co	Ni	Cr	Fe	Mo	W	P	V
26-VTM	2	.07	<.1	<.1	8.90	Bal	12.35	.06	1.87	3.91	.001	
OR 11148												

CHEMICAL ANALYSIS												
%	No. of Pcs	Ti	Al	Cr	Ta	B	S	Cu	Zr	Al+Ti	Nv	
26-VTM	.2	4.00	3.37	<.1	4.01	.015	.0010		.02	7.37	2.24	

Pb < 1 ppm Bi < .3 ppm Ag < 5 ppm

MECHANICAL TESTS												
ATOR Y NO.	TEST TEMP. °F	TENSILE STRENGTH PSI	Y.S. 0.2% OFFSET PSI	Y.S. 0.02% OFFSET PSI	RUPTURE STRESS PSI	RUPTURE LIFE HRS.	ELONG. INT'	R.A. %	GRAIN SIZE	I.O.A.	HARDNESS ROCKWELL C	AS CAST
26-VTM	75	163,000	141,000				6.3	7.8				
	1200	169,000	124,000				8.7	8.6				

Chemical analysis obtained from a cast test coupon from the indicated master heat. Mechanical test results obtained from bars machined from part number 161415, Serial No. A003, Hip Lot No. 81-334 and heat treated to specification requirements. Testing source: Howmet Turbine Components Corporation, Technical Center, Whitehall, MI. Master heat source: Howmet Turbine Components Corporation, Alloy Division, Dover, N.J. Master heat no. 113B11J48

THIS HEAT HAS BEEN ANALYZED FOR THE FOLLOWING ELEMENTS NOT LISTED IN MATERIAL SPECIFICATION.  
 Ag <.01% Se .5 ppm Te <.5 ppm Ti <.5 ppm

December 11, 1981

SUBSCRIBED AND SWEORN TO BEFORE ME

*H. J. DeLong*

NOTARY PUBLIC

MY COMMISSION EXPIRES

AUTHORIZED SIGNATURE

*H. J. DeLong*

January 28, 1984

**APPENDIX B**

**MECHANICAL AND AERODYNAMIC DESIGN  
VERIFICATION TEST PLAN - MTR MONOROTOR**

Spin testing will be conducted in the spin pit fixture (Drawing 161786). The monorotor and shaft assembly will be mounted in a modified T-20G bearing capsule and coupled to the spin pit drive turbine. Two proximity probes are positioned 90 degrees apart at the exducer hub to measure shaft motion during transient acceleration and decelerations.

Brittle lacquer stress coating will be conducted with residual bearing oil only to minimize the possibility of oil contaminating the lacquer. This will be possible as coating stress cracks should occur at low (approximately 25 percent design) speed.

### B.1 SPIN PIT TEST PROCEDURE

Spin pit testing will commence according to the following procedure:

1. Place stress coated monorotor in spin pit fixture and couple to spin pit drive turbine. Photograph monorotor and spin head.
2. Connect all instrumentation and record proximity probe output on tape and oscilloscope.
3. Accelerate past the first critical speed to 15 percent design speed and immediately shut down.
4. Examine and pre-analyze test data for accuracy and trend.
5. Accelerate to 20 percent design speed shutdown and inspect for cracks. Repeat in additional one percent increments until lacquer cracks are discerned.
6. Conduct steady acceleration to 100 percent design speed monitoring proximity probe output. Shut down, inspect, and pre-analyze data.

7. Contingent upon completing Step 6, accelerate to 120 percent design speed and repeat three times.

8. Determine maximum speed capability of spin head and monorotor.

## B.2 AERODYNAMIC DESIGN VERIFICATION (OPTIONAL)

An existing T-20G gas turbine baseline engine will be modified to accept one of the mid-temperature turbine monorotors for performance evaluation purposes. As the degree of modification is highly dependent upon operating turbine inlet temperature, initial plans will be to conduct turbine testing at short time turbine inlet temperatures no higher than currently attainable with existing hardware (1800 to 1900°F). As a minimum, the following instrumentation will be installed to determine component performance:

- Turbine inlet total temperature
- Turbine inlet total pressure
- Turbine inlet flow
- Turbine exit total pressure
- Turbine exit static pressure
- Turbine exit total temperature
- Turbine rotational speed
- Turbine output power

Engine test performance will be obtained at 93 and 100 percent design corrected speed (100 percent = 93,500 rpm) at a minimum of six turbine inlet temperatures equally spaced between no load and maximum turbine inlet temperature. The engine test data will be analyzed to determine overall engine, compressor, and turbine performances.

Subsequent to the performance evaluation, the turbine will be examined to determine its mechanical conditions. A short endurance demonstration run will then be commenced at the following conditions:

- 100 Percent Mechanical Speed
- 20 Cycles - Each cycle consisting of:
  - 5 minutes no load
  - 5 minutes half load
  - 5 minutes full load (maximum turbine inlet temperature)
  - 5 minutes shut down

The engine will be subsequently disassembled to carry out a thorough mechanical inspection of the turbine components.

A Phase III Test Report will be prepared covering all test work, test analysis, test data compilation, and component examination.

## **APPENDIX C**

### **ALTERNATE BALANCE PROCEDURE FOR SUGGESTED MONOROTOR**

### C.1 BACKGROUND

The first monorotor assembly was received at Turbomach in the final machined condition, but not balanced. Its initial unbalance of 0.236 in.-oz. seemed excessive. Calculating the unbalance permitted by drawing tolerances showed that the rotor could be as much as 0.518 in.-oz. out of balance and still meet print runout requirements. Material removal areas shown on the print were insufficient to achieve balance; so new material removal areas were suggested which permitted removal of blade tips and disk rim material.

### C.2 NEED

To avoid removing large quantities of material, an alternate balance method which would eliminate most of the unbalance during the machining process would be desirable. In simple terms, to produce a monorotor assembly which has little unbalance, the bearing race diameters would be machined on the same axis as the center of mass of the rotor.

### C.3 APPROACH

This suggestion is an attempt to find the mass center of the rotor assembly prior to final machining so that final diameters of the shaft will be coaxial with the mass center.

The sequence of operations would be:

1. Inertia weld raw 4340 bar stock to rotor casting as currently defined, permitting reasonable concentricity tolerance.
2. Create a rotor axis by machining center points in each end of the welded assembly.

3. Machine the assembly to a semi-finished configuration with all diameters approximately 0.040 or 0.050 larger than their final size.  
(Note: A new drawing may be necessary to define the semi-machined configuration.) Figure C-1 shows the semi-machined shape in phantom lines.
4. Check balance the rotor on its axis. Determine the amount of unbalance and its direction by direct readings from the balance machine or by placing wax on blade tips to achieve balance.

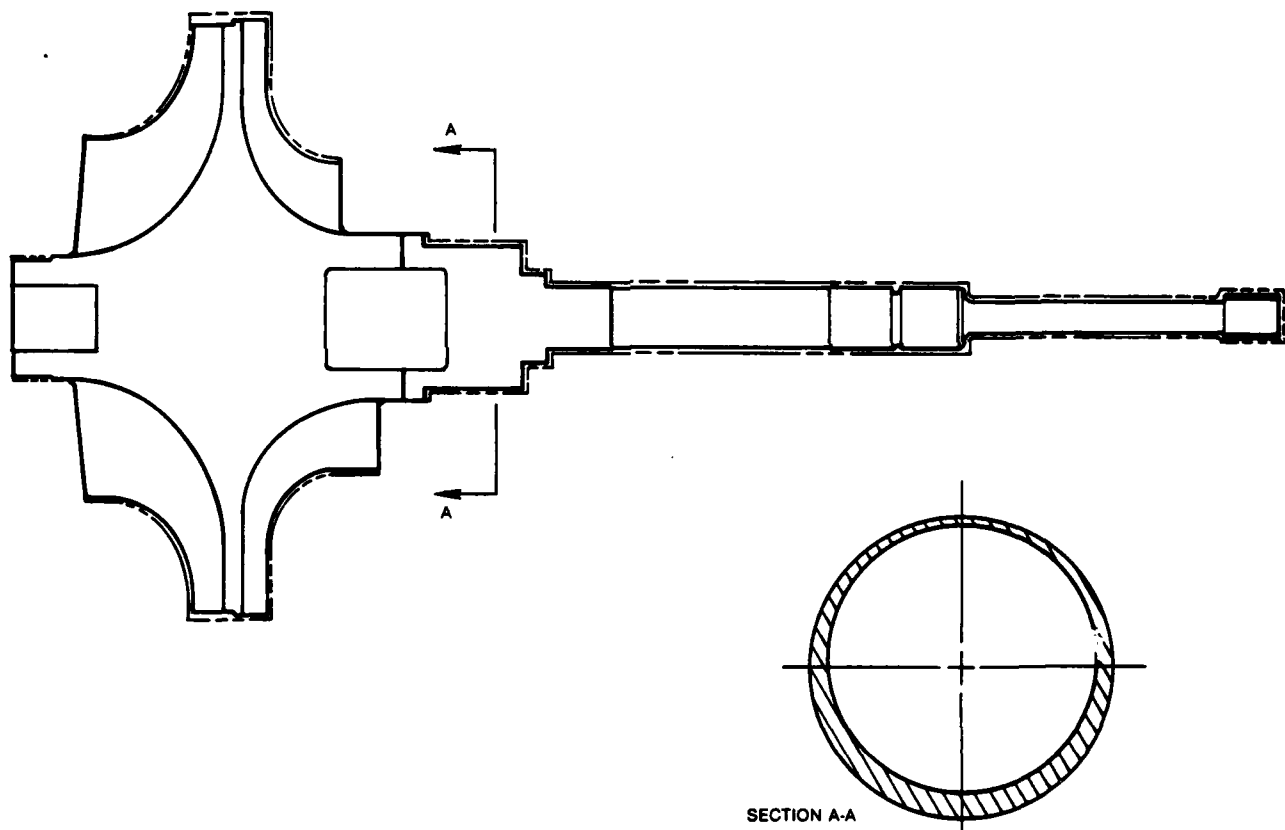


Figure C-1. Semi-Machined Shape

5. Using the following equation, calculate the distance from the axis to the rotor mass center:

$$d_c = \frac{U}{W_r}$$

where:  $d_c$  = distance from axis to mass center

$U$  = unbalance of semi-finished rotor in units of inch-ounces

$W_r$  = semi-furnished rotor assembly weight in ounces

6. If the rotor axis were moved by an amount " $d_c'$ " (by creating new machine centers), the semi-finished rotor would be balanced. However, Section A-A of Figure C-1 shows that after moving the rotor axis, the material removed during the final machining will be eccentric, thus inducing unbalance. Sections C.4 and C.5 show the derivation of a factor used to account for this secondary balance requirement and the modified equation becomes:

$$d_c' = \frac{U}{W_r} \left( \frac{W_r - 2}{W_r + 24.5} \right)$$

where:  $W_t$  = weight of material removed in final machining:  
Approximately 2 oz.

$U'$  = unbalance induced by eccentric machining: Approximately  
26.5 in.-oz.  
in.

7. With caution and accuracy, grind new machine centers in both ends of the semi-finished rotor which are displaced from the original centers a distance " $d_c$ " in the direction of unbalance.
8. Using new centers, finish machine the assembly per drawing requirements. The finished rotor will have relatively little static unbalance.

Several basic assumptions were made in developing this concept:

- Methods are available to grind new machine centers at an accurate distance from old ones (tolerances of 0.001 or less).
- A new center can be created near an old one without the tool wandering into the original center.
- The added cost of producing the semi-machined rotor will not be prohibitive.
- Dynamic balance will be easy to achieve if static unbalance is low.

If any of these assumptions are erroneous, then the original method of removing material from blade tips or disk rim will have to be used. It should be pointed out, however, that a check balance after rough machining will be valuable. If the part is highly unbalanced, the center axis could be corrected as described above before final machining. If the rough machined part has only low or moderate unbalance, simply finish the rotor assembly and then balance it by material removal.

A development program to establish the workability of balancing during manufacture rather than balancing by material removal will be valuable to the monorotor program as well as future programs.

DEFINITION OF DISTANCE TO MACHINING CENTER HAVING A FACTOR WHICH ACCOUNTS FOR ECONOMICITY OF MATERIAL REMOVAL AS WELL AS A FACTOR FOR INITIAL UNBALANCE.

#### NOMENCLATURE:

$d_c'$  = MODIFIED DISTANCE TO MACHINING CENTER.

$U$  = UNBALANCE OF SEMI-FINISHED ROTOR DETERMINED BY BALANCE MACHINE

$U'$  = UNBALANCE FACTOR BASED ON WEIGHT OF FINISHED ROTOR.

$W_r$  = WEIGHT OF SEMI-FINISHED ROTOR

$W_t$  = WEIGHT REMOVED DURING FINAL MACHINING

EQUATION FOR  $d_c'$  IS:

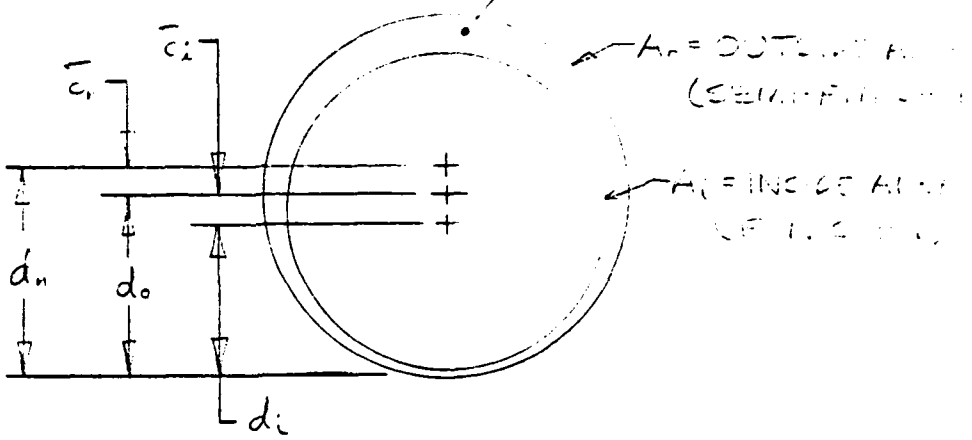
$$d_c' = \frac{U}{W_r} - \frac{U'd_c'}{W_r - W_t} \Rightarrow d_c' \left( 1 + \frac{U'}{W_r - W_t} \right) = \frac{U}{W_r}$$

$$d_c' \left( \frac{W_r - W_t + U'}{W_r - W_t} \right) = \frac{U}{W_r}$$

$$d_c' = \frac{U}{W_r} \left( \frac{W_r - W_t}{W_r - W_t + U'} \right)$$

$U$  AND  $W_r$  WILL BE DETERMINED EMPIRICALLY FOR EACH ROTOR AS IT IS PRODUCED, BUT  $U'$  AND  $W_t$  SHALL BE APPROXIMATED IN THE FOLLOWING MANNER.

### 3.5 CALCULATION



$$A_o = \frac{\pi D_o^2}{4}, \quad A_i = \frac{\pi D_i^2}{4}, \quad A_n = A_o - A_i$$

$$d_o = \frac{D_o}{2}; \quad c_i = \frac{D_o}{2} - \bar{c}_i, \quad d_n = \frac{D_o}{2} + \bar{c}_n \Rightarrow \bar{c}_n = d_n - \frac{D_o}{2}$$

$$\text{EQ1)} \quad A_o d_o - A_i d_i = A_n d_n \Rightarrow d_n = \frac{A_o d_o - A_i d_i}{A_o - A_i}$$

$$d_n = \frac{\left(\frac{\pi D_o^2}{4}\right)\left(\frac{D_o}{2}\right) - \left(\frac{\pi D_i^2}{4}\right)\left(\frac{D_o}{2} - \bar{c}_i\right)}{\frac{\pi D_o^2}{4} - \frac{\pi D_i^2}{4}} = \frac{\frac{D_o^3}{2} - \frac{D_o^2 D_i}{2} + D_i^2 \bar{c}_i}{D_o^2 - D_i^2}$$

$$\text{EQ2)} \quad \bar{c}_n = d_n - \frac{D_o}{2} = \left[ \frac{\frac{D_o^3}{2} - \frac{D_o^2 D_i}{2} + D_i^2 \bar{c}_i}{D_o^2 - D_i^2} \right] - \frac{D_o}{2} = \frac{D_i^2 \bar{c}_i}{D_o^2 - D_i^2}$$

$$\text{EQ3)} \quad W_n = \left( \frac{\pi D_o^2}{4} - \frac{\pi D_i^2}{4} \right) L \rho = \frac{\pi}{4} \rho L (D_o^2 - D_i^2)$$

COMBINE EQUATIONS 2 AND 3:

$$\text{EQ4)} \quad W_n \bar{c}_n = \frac{\pi}{4} \rho L (D_o^2 - D_i^2) \left( \frac{D_i^2 \bar{c}_i}{D_o^2 - D_i^2} \right) = \frac{\pi}{4} \rho L D_i^2 \bar{c}_i$$

$$W_n \bar{c}_i = \frac{\pi}{4} L - D_i^2 \bar{c}_i$$

WE ARE ASSUMING THAT ALL FEATURES OF THE  
SHAFT ARE IDENTICAL, AND WE USE THE SAME APPROXIMATION  
FOR DIFFERENT DIAMETERS ALONG THE LENGTH OF THE  
SHAFT, EXCEPT THAT IT MUST BE APPLIED TO EACH  
DIAMETER SEPARATELY.

$$\Sigma W_n \bar{\Sigma}_n = \frac{\pi}{4} \rho \bar{\delta}_c (D_1^2 L_1 + D_2^2 L_2 + D_3^2 L_3 + \dots)$$

### C.E.1 DETERMINE APPROXIMATE NUMBER FOR UNEALANCE INDUCED BY ECCENTRIC MACHINING

SHAFT		
$D_i$	$L$	$D_i^2 L$
0.344	0.42	0.0497
0.153	2.00	0.1280
0.466	0.50	0.1086
0.415	0.06	0.0163
0.4784	0.51	0.1132
0.465	1.92	0.4024
0.4724	0.51	0.1132
0.422	0.18	0.0852
1.0782	0.775	0.9513
$\sum D_i^2 L =$		1.9491

$$\frac{\pi}{4} \rho \bar{\delta}_c = \frac{\pi}{4} (0.283)(16) \bar{\delta}_c$$

$$\frac{\pi}{4} \rho \bar{\delta}_c = 3.56 \bar{\delta}_c$$

$$\sum_{\text{SHAFT}} W_n \bar{\Sigma}_n = 3.56 \bar{\delta}_c (1.9491) = 6.932 \bar{\delta}_c$$

$$\sum_{\text{ROTOR}} W_n \bar{\Sigma}_n = 3.76 \bar{\delta}_c (5.2022) = 19.549 \bar{\delta}_c$$

$$\sum_{\text{TOTAL}} W_n \bar{\Sigma}_n = 26.481 \bar{\delta}_c$$

THEREFORE:

$$U' = \frac{\sum W_n \bar{\Sigma}_n}{\text{NUMBER OF ELEMENTS}}$$

C.E.2 DETERMINE WEIGHT OF MACHINING  
REMOVED BETW. EEE. PROD. MACHINING  
AND FINAL MACHINING.

$$W_t = \frac{\pi}{4} \rho (D_o^2 - D_i^2) L$$

	SHAFT			ROTOR		
$D_o$	$D_i$	$L$	$(D_o^2 - D_i^2)L$			
0.374	0.344	0.42	0.0122	COMP TIP =	$(0.21)(0.02)(0.1)(16) = .0067$	
0.373	0.253	2.00	0.0437	" "	$(1.00)(0.02)(0.1)(16) = .032$	
0.371	0.326	0.50	0.0225	TURB TIP =	$(0.21)(0.02)(0.045)(16) = .0017$	
0.372	0.475	0.06	0.0054	" "	$(1.20)(0.02)(0.1)(16) = .034$	
0.371	0.4724	0.51	0.0199	DISK RIM =	$(\pi/4)(4.59^2 - 4.55^2)(.06) = .0171$	
0.372	0.460	1.93	0.0775	" "	$(\pi/4)(4.59^2 - 4.20^2)(1.00) = .567$	
0.371	0.4724	0.51	0.0199	AFT DIA =	$(\pi/4)(9.65^2 - 7.05^2)(.06) = .311$	
0.372	0.387	0.17	0.0102			
1.132	1.0762	0.775	0.0681			
			<u>.2002</u>			
			$W_{t,SHAFT} = \frac{\pi}{4} (.28)(16)(.3002)$			
					$W_{t,ROTOR} = \rho (.1807) = .8645$	
			$W_{t,SHAFT} = 1.0674 \text{ oz}$			
						<u>.1807</u>

$$W_t,SHAFT = \frac{\pi}{4} (.28)(16)(.3002)$$

$$W_t,SHAFT = 1.0674 \text{ oz}$$

$$W_t = W_t,SHAFT + W_t,ROTOR = 1.0674 + .8645$$

$$W_t = 1.9319 \text{ oz} \approx 2 \text{ oz.}$$

C.E.3 FINAL EQUATION FOR MOVING  
CENTER TO ESTABLISH BALANCE

$$d_c' = \frac{u}{w_r} \left( \frac{w_r - v_r}{v_r - l_c + u} \right) = \frac{u}{w_r} \left( \frac{w_r - 2}{w_r - 2 + 24.5} \right)$$

$$d_c' = \frac{u}{w_r} \left( \frac{w_r - 2}{w_r + 24.5} \right)$$

**END**

**FILMED**

**7-83**